An Extension of a Kinetic Theory of Polymer Crystallization through the Exclusion of Negative Barriers

Jerry I. Scheinbeim, Louis Petrone, and Brian A. Newman*

Department of Mechanics and Materials Science, Rutgers University, Piscataway, New Jersey 08855-0909

Received March 12, 1991; Revised Manuscript Received September 29, 1992

ABSTRACT: The simplest version of the Lauritzen–Hoffman (LH) model of polymer crystallization, which applies to infinitely long model polymer molecules crystallizing on an existing substrate of infinite width, is reexamined. The mathematical expressions for the model free energy barriers are observed to take on negative values at high supercooling. Since such negative barriers appear to be physically unrealizable for the crystallization process, the LH model is extended by imposing a mathematical constraint on the expressions for the barriers, to forbid them from ever being negative. The extended model contains one parameter γ which varies from 0 to 1 and is analogous to the parameter ψ of the LH model. For all values of γ less than 1, the extended model predicts a finite lamellar thickness at every supercooling; moreover, this thickness, at large undercooling, decreases monotonically with increasing undercooling, in agreement with experiment but in marked contrast to the LH model which exhibits the well-known δl catastrophe. The relative insensitivity of the calculated lamellar thicknesses to the parameter γ supports the use of $\gamma = 0$ as a first approximation for mathematical convenience in practice.

I. Introduction

Recently, the crystallization of poly(vinylidene fluoride) (PVF_2) in the presence of high electric fields has been studied both experimentally and theoretically. Of the four well-known crystalline forms α, β, γ, and δ (or II, I, III, and IV) of PVF_2, the phase with the largest spontaneous polarization and potential for applications is the β-phase. Crystallization of PVF_2 from a concentrated solution of tricresyl phosphate in the presence of a high electric field was observed[1] to produce β-phase crystals, with dipoles oriented in the field direction, during the initial stages of crystallization followed by the growth of unoriented α-phase crystals (nonpolar) as crystallinity increased and the tricresyl phosphate content decreased by evaporation. The decrease in tricresyl phosphate content and subsequent crystal growth behavior suggests that the local electric field in the solution region changes. Other experimental and theoretical[2,3] studies of crystallization of PVF_2 from the melt in the presence of a high static electric field have been made and were found to give γ-phase crystals which however did not show crystal orientation. As part of the continuing effort to understand the structure–property relationships of PVF_2 and because of its practical importance, our ultimate goal—despite the complexity of the system described—is to develop a theory or model which can account for its crystallization behavior from concentrated solutions in the presence of an electric field.

As in the case of isothermal crystallization of α- and γ-phases from the melt in an electric field,[3] a theory of isothermal crystallization of α-, β-, and δ-phases from concentrated solution in an electric field would be based on "classical" and "polymer" theories of nucleation and growth in the absence of an applied field. Most importantly, the nucleation barrier or activation free energy barrier for nucleation would certainly be different in the presence of the field than in its absence; and this barrier has been seen to be of fundamental importance in the theories of polymer crystallization, the simplest of which is the LH or Lauritzen–Hoffman theory.[4,5] One possibly unrealistic feature which seems to have been incorporated into the LH theory in order to simplify it is that the nucleation barrier is not constrained in the theory to take on only nonnegative values.[6] The word "barrier" connotes a positive quantity, and, furthermore, the LH theory is based on transition state theory in which the barrier corresponds to an intermediate configuration or transition state of the system which is at a free energy maximum relative to some initial and final states of the system.[9] Moreover, the LH theory exhibits, in contrast with experiment, the δl catastrophe wherein the calculated average lamellar thickness $\bar{l}$ suddenly passes through a minimum and becomes infinite at a temperature T_c, corresponding to a moderately large undercooling; and, in fact, the nucleation barrier in this theory is positive for all $T > T_c$, is zero at $T = T_c$, and is negative for all $T < T_c$ for the special case which Lauritzen and Hoffman[4,5] have recently considered. Therefore, prior to developing an extension of the LH theory which would involve ascertaining the effect of an electric field on the nucleation barrier, we try to extend the LH theory to larger undercooling by incorporating into it the assumption that free energy barriers cannot be negative. Note that, unlike in the LH theory of polymer crystallization, barriers in classical nucleation theory are never negative; however, the classical theory does not explicitly take into account polymer chain folding, and, for that reason, we have not yet considered modifying the Marand and Stein theory[2] of crystallization from the melt to treat the PVF_2/tricresyl phosphate crystallizing solution.

The remainder of this paper is organized as follows. In section II, the LH model is described. The kinetic treatment of the LH model is given in section III. The rate constants needed for this treatment are determined in section IV. Next, our extension of the LH model is described in section V; the conditions which determine the sign of $\Delta\phi_1$, the free energy of formation of that portion of a model polymer molecule which crystallizes first on an existing crystal, are found in section VI. A summary of the expressions for the barriers in our model is given in section VII along with the expressions for the average lamellar thickness. In section VIII, the variable transformations required as a preliminary to numerical integration are introduced. Results and discussion appear in section IX, and conclusions are given in section X.

II. The Lauritzen–Hoffman Model

The model to be extended is one version[4,5] of the well-known Lauritzen–Hoffman (LH) model of polymer crys-

0024-9297/93/2226-0933$04.00/0

tallization. Our description of this version is as follows. The model polymer molecules are assumed to be infinitely long and crystallize on an existing crystalline face or substrate which is assumed to be infinitely wide (i.e., the fact that its width is finite is ignored). A sequence of length l of polymer segments of width a and thickness b as well as the volume associated with that sequence—which is taken to be a parallelepiped of length l, width a, and thickness b—is designated as a stem. Only stems of length l can crystallize on an existing face of length l, but the length l, the lamellar thickness, can vary from crystal to crystal. *Any* sequence of length l of segments of a model molecule can be placed first on a given face and, upon placement, is designated as the first stem. The free energy of formation of the first stem is

$$\Delta\phi_1 - \Delta\phi_0 \equiv \Delta\phi_1 - 0 \quad \text{or} \quad \Delta\phi_1 = 2ab\sigma_e' + 2bl\sigma - abl\Delta f$$

where $\Delta f > 0$ is the free energy of fusion per unit volume at a temperature T below the melting point T_m° of the model polymer (i.e., of a crystal of very large l) and $\Delta f = 0$ at $T = T_m^\circ$; where σ is the lateral surface free energy per unit area (i.e., that associated with the surfaces of area bl and al of a stem); and where σ_e' is the surface free energy per unit area associated with the cilium that protrudes through each of the surfaces of area ab of the first stem. Recently,[4-7] σ_e' has been assumed to be zero; generally, one can assume[11] that $0 \le \sigma_e' \le \sigma_e$. All surface free energies per unit area in the model are assumed to be independent of T and l. (See Figure 2a of ref 4 or Figure 22 of ref 5.) The placement of each subsequent stem involves (1) the destruction of the cilium associated with one of the surfaces of area ab of an adjacent stem already crystallized, (2) an adjacent reentry and the formation of a tight fold associated with two surfaces of area ab, and (3) the formation of a cilium associated with the remaining surface of area ab of the stem being placed. Only adjacent reentry and hence only tight folding is incorporated in this version of the model.

The free energy of formation of the νth stem ($\nu > 1$) is therefore

$$\Delta\phi_\nu - \Delta\phi_{\nu-1} = -ab\sigma_e' + 2ab\sigma_e + ab\sigma_e' - abl\Delta f$$

or

$$\Delta\phi_\nu - \Delta\phi_{\nu-1} = 2ab\sigma_e - abl\Delta f \equiv -E$$

where $\Delta\phi_\nu$ is the free energy of formation of a group of ν stems (relative to $\Delta\phi_0 = 0$) where σ_e is the surface free energy per unit area associated with half of a fold. Iteration of $\Delta\phi_\nu = \Delta\phi_{\nu-1} - E$ ($\nu > 1$) gives

$$\begin{aligned}\Delta\phi_\nu &= \Delta\phi_1 - (\nu-1)E \\ &= 2bl\sigma + 2ab\sigma_e' - 2ab\sigma_e + \nu ab(2\sigma_e - l\Delta f)\end{aligned}$$

In order that stem additions subsequent to the placement of the first stem be thermodynamically favorable, i.e., in order that they would in fact occur, one must impose the constraint $-E < 0$ and consequently $l > 2\sigma_e/\Delta f$. Stems of smaller length are unstable and disappear. By contrast, $\Delta\phi_1$ can be positive, zero, or negative; $E > 0$ guarantees that $\Delta\phi_\nu < 0$ will occur for finite ν. Note the sign conventions for $\Delta\phi_1$ and E.

III. Kinetic Treatment of the Lauritzen–Hoffman Model

Our description of the kinetic treatment[4,5] of the LH model is as follows. The following assumptions are made:

1. Assume that transition state theory can be utilized to describe the kinetics of the LH model of polymer crystallization.

2. Assume that the formation (crystallization) of a single stem is an elementary process or elementary reaction, that the destruction (melting) of a single stem is an elementary process or elementary reaction, and that transition state theory can be applied to these two elementary processes with a single transition state corresponding to a relative free energy maximum or barrier thus occurring between each two integral values of ν on a plot of $\Delta\phi_\nu$ vs ν.

3. Assume that only one stem at a time can be formed or destroyed.

The kinetic problem is to derive an expression for the net rate $S_\nu(l,T)$ at which stems of length l (and width a) pass over or surmount the νth free energy barrier at temperature T. The problem requires consideration of the set of connected elementary reactions

$$0 \underset{B_1}{\overset{A_0}{\rightleftarrows}} 1 \underset{B}{\overset{A}{\rightleftarrows}} 2 \underset{B}{\overset{A}{\rightleftarrows}} 3 \underset{B}{\overset{A}{\rightleftarrows}} 4 \ldots$$

where A is the rate constant for the forward reaction $\nu \rightarrow \nu + 1$ ($\nu \ge 1$) and B is that for the reverse reaction $\nu + 1 \rightarrow \nu$ ($\nu \ge 1$), and where A_0 and B_1 are the analogous rate constants for the $\nu = 0 \rightleftarrows \nu = 1$ reactions. Solution of this problem in the steady-state approximation gives

$$S_\nu(l,T) = \frac{N_0 A_0 (A - B)}{A - B + B_1} \equiv S(l,T)$$

for all ν, where N_0 is the number of sites or locations available for the placement of a first stem. The total net rate at which stems (i.e., the net rate including stems of all possible values of l) pass over the νth barrier at temperature T is given, for all ν, by

$$S_{\text{Total}}(T) = \sum_{l=l_1}^{\infty} S(l,T)$$

where l_1 is the smallest allowed value of l which satisfies the constraint $l > 2\sigma_e/\Delta f$. Note that l is a discrete variable—the smallest increment in l that can be made is the monomer repeat length l_u. To find l_1, first write $l = ml_u$, where m is a positive integer. Then $l > 2\sigma_e/\Delta f$ implies $m > (2\sigma_e/\Delta f)/l_u$; that is, m is greater than or equal to the smallest integer greater than $(2\sigma_e/\Delta f)/l_u$, and, therefore, $l_1 = [1 + \text{INT}(X)]l_u$, where $X \equiv (2\sigma_e/\Delta f)/l_u$ and $\text{INT}(X)$ designates the integer part of X. Substituting $l_u = 2\sigma_e/X\Delta f$ into the expression for l_1 gives $l_1 = [(1 + \text{INT}(X))/X](2\sigma_e/\Delta f)$. To a good approximation, $(1 + \text{INT}(X))/X \approx 1$ (i.e., X is sufficiently greater than 1) so that $l_1 \approx 2\sigma_e/\Delta f$.

Finally, one assumes that $\sum_{l=l_1}^{\infty} S(l,T) \approx 1/l_u \int_{l_1}^{\infty} S(l,T)\,dl$; and the kinetically-determined average lamellar thickness is then given by

$$\bar{l}(T) = \frac{\int_{l_1}^{\infty} lS(l,T)\,dl}{\int_{l_1}^{\infty} S(l,T)\,dl}$$

IV. Determination of the Rate Constants

To obtain expressions for A_0, B_1, A, and B, one must first determine expressions for the free energy barriers for the relevant reactions $\nu \rightleftarrows \nu + 1$ ($\nu \ge 0$). Let E_1 be the free energy barrier to the destruction of the first stem; then $\Delta\phi_1 + E_1$ is the barrier to the formation of the first stem in order that $(\Delta\phi_1 + E_1) - E_1 = \Delta\phi_1$. Let E_2 be the free energy barrier to the formation of each subsequent stem; then $E + E_2$ is the barrier to the destruction of each such stem in order that $(E + E_2) - E_2 = E$. Now, one does not know the free energy barrier to the formation of the first

stem. At least, one does know that it depends on what length l' of a fully adsorbed stem of length l actually crystallizes before the barrier is surmounted. If $l' = 0$, then none of the free energy of crystallization (i.e., $-abl\Delta f$) is released before the barrier is surmounted, and clearly, $\Delta\phi_1 + E_1 = 2ab\sigma_e' + 2bl\sigma$ and $E_1 = abl\Delta f$. In general, then, for $0 \le l' \le l$

$$\Delta\phi_1 + E_1 = 2ab\sigma_e' + 2bl\sigma - abl'\Delta f \quad \text{and}$$

$$E_1 = ab(l - l')\Delta f$$

Since l' is unknown, a parameter $\psi \equiv l'/l$ with $0 \le \psi \le 1$ is introduced in order that all possible so-called apportionments of the free energy of fusion $abl\Delta f$ between the rate constants for the formation and destruction of a first stem (i.e., for the forward and reverse reactions $0 \rightleftarrows 1$) can be considered. Thus

$$\Delta\phi_1 + E_1 = 2ab\sigma_e' + 2bl\sigma - \psi abl\Delta f \quad \text{and}$$

$$E_1 = (1 - \psi)abl\Delta f.$$

Note that the greater the amount $\psi abl\Delta f$ of the free energy of fusion which is in fact "apportioned" (i.e., the greater the value of ψ or l'), the smaller the value of both $\Delta\phi_1 + E_1$ and E_1 (for a given l and T). A very similar interpretation of ψ has been discussed recently.[7]

Similarly, for each subsequent stem, let l'' ($0 \le l'' \le l$) be the length of a fully adsorbed stem which actually crystallizes before the barrier to the formation of the stem is surmounted. Then

$$E_2 = 2ab\sigma_e - abl''\Delta f \quad \text{and} \quad E + E_2 = ab(l - l'')\Delta f$$

Define the apportionment parameter $\hat{\psi} \equiv l''/l$ with $0 \le \hat{\psi} \le 1$ so that

$$E_2 = 2ab\sigma_e - \hat{\psi}abl\Delta f \quad \text{and} \quad E + E_2 = (1 - \hat{\psi})abl\Delta f.$$

Finally, utilizing transition state theory

$$A_0 = \frac{kT}{h}e^{-(\Delta\phi_1 + E_1 + \Delta\hat{F})/kT} \equiv \beta e^{-(\Delta\phi_1 + E_1)/kT}$$

$$B_1 = \beta e^{-E_1/kT}; \quad A = \beta e^{-E_2/kT}; \quad B = \beta e^{-(E+E_2)/kT}$$

where $\Delta\hat{F}$ is the contribution to *each* barrier as a result of retardations in the transport of a polymer chain through the liquid to the substrate or vice versa. Note that B/A does not depend on $\hat{\psi}$ and that B_1/A_0 does not depend on ψ as required.

V. Extension of the Lauritzen–Hoffman Model

As implied throughout the above discussion, the application of transition state theory to the elementary processes of single stem formation and destruction presumes that there is a single relative free energy maximum[9] or barrier between each two integral values of ν on a plot of $\Delta\phi_\nu$ vs ν. Consequently, $\Delta\phi_1 + E_1$, E_1, E_2, and $E + E_2$ should never be negative. Clearly, $E_1 = (1 - \psi)abl\Delta f$ and $E + E_2 = (1 - \hat{\psi})abl\Delta f$ are never negative; however, the expressions given above for $\Delta\phi_1 + E_1$ and E_2 can be negative. In fact, E_2, for example, is negative for all l such that $2\sigma_e/\hat{\psi}\Delta f < l$ for a given Δf, $\hat{\psi}$, and σ_e. We propose to extend the LH model by incorporating into the model the assumption that free energy barriers cannot be negative; i.e., only apportionments of the free energy of fusion which result in a nonnegative barrier will be allowed.

In order to incorporate this constraint into the model, first note that $\Delta\phi_1 + E_1 = 2ab\sigma_e' + 2bl\sigma - \psi abl\Delta f$ is never negative when $\Delta\phi_1$ is positive since then $abl\Delta f < 2ab\sigma_e' + 2bl\sigma$ always holds and $\psi abl\Delta f < 2ab\sigma_e' + 2bl\sigma$ follows. However, when $\Delta\phi_1$ is negative, the expression $2ab\sigma_e' + 2bl\sigma - \psi abl\Delta f$ can be negative. The requirement that $\Delta\phi_1 + E_1 \ge 0$ hold when $\Delta\phi_1$ is negative implies that one is not allowed to apportion all of the free energy of fusion $abl\Delta f$ when $\Delta\phi_1$ is negative. If the amount $\psi abl\Delta f$ of the free energy of fusion which is apportioned were to exceed $2ab\sigma_e' + 2bl\sigma$, then $\Delta\phi_1 + E_1$ would be negative. The maximum amount which can be apportioned is indeed $2ab\sigma_e' + 2bl\sigma$, and therefore one has, when $\Delta\phi_1 < 0$

$$\Delta\phi_1 + E_1 = \xi(2ab\sigma_e' + 2bl\sigma)$$

where ξ is an apportionment parameter with $0 \le \xi \le 1$. Using $(\Delta\phi_1 + E_1) - E_1 = \Delta\phi_1$ or $E_1 = (\Delta\phi_1 + E_1) - \Delta\phi_1$ gives

$$E_1 = \xi(2ab\sigma_e' + 2bl\sigma) - (2ab\sigma_e' + 2bl\sigma - abl\Delta f) =$$

$$abl\Delta f - (1 - \xi)(2ab\sigma_e' + 2bl\sigma)$$

Observe that the requirement that $\Delta\phi_1 + E_1 \ge 0$ holds when $\Delta\phi_1$ is negative is equivalent to the physically realistic requirement that the barrier E_1 to the destruction of the first stem cannot be smaller than the free energy increase $(-\Delta\phi_1)$ that occurs upon its destruction. Note that $abl\Delta f - (2ab\sigma_e' + 2bl\sigma) = -\Delta\phi_1$. Also, this physically realistic requirement implies that an adsorbed first stem cannot completely crystallize before the barrier to the formation of that stem is surmounted, i.e., that the upper limit on l' is less than l when $\Delta\phi_1$ is negative. This upper limit on l' is determined later. For $\Delta\phi_1 > 0$, the expressions $\Delta\phi_1 + E_1 = 2ab\sigma_e' + 2bl\sigma + \psi abl\Delta f$ and $E_1 = (1 - \psi)abl\Delta f$ still hold with $0 \le \psi \le 1$ and $0 \le l' \le l$.

At this point, a simple change of variable is introduced for convenience. Define $\lambda \equiv 1 - \xi$ with $0 \le \lambda \le 1$.

Now observe that, although the free energy of fusion is $abl\Delta f$ when $\Delta\phi_1$ is positive or negative, the free energy of fusion which can be apportioned is $abl\Delta f$ when $\Delta\phi_1$ is positive but is $(2ab\sigma_e' + 2bl\sigma)$ when $\Delta\phi_1$ is negative. Also, the free energy of fusion that is in fact apportioned is $\psi abl\Delta f$ when $\Delta\phi_1$ is positive but is $\lambda(2ab\sigma_e' + 2bl\sigma)$ when $\Delta\phi_1$ is negative. Clearly then, the fraction of the free energy of fusion which can be apportioned that is apportioned is ψ when $\Delta\phi_1$ is positive but is λ when $\Delta\phi_1$ is negative. If we always choose the same value for λ and ψ, then, over the whole range of values for $\Delta\phi_1$, the fraction of the free energy of fusion which can be apportioned has the same value. Let γ denote any particular value which is chosen for both ψ and λ, where $0 \le \gamma \le 1$.

Note that equal values of ψ and λ do *not* imply the same value of l' (except when $\Delta\phi_1 = 0$, as will become evident); as usual $\psi \equiv l'/l$ but an expression for λ in terms of l' or vice versa remains to be obtained. In our approach, then, l' depends at least on the sign of $\Delta\phi_1$, and yet we utilize only one parameter, γ—the fraction of the free energy of fusion which can be apportioned that is apportioned—which is a constant over the whole range of values for $\Delta\phi_1$.

In summary, the barriers in terms of the apportionment parameter γ are

$$\left.\begin{aligned}\Delta\phi_1 + E_1 &= (1 - \gamma)(2ab\sigma_e' + 2bl\sigma)\\ E_1 &= abl\Delta f - \gamma(2ab\sigma_e' + 2bl\sigma)\end{aligned}\right\} \quad \text{for } \Delta\phi_1 \le 0$$

$$\left.\begin{aligned}\Delta\phi_1 + E_1 &= 2ab\sigma_e' + 2bl\sigma - \gamma abl\Delta f\\ E_1 &= (1 - \gamma)abl\Delta f\end{aligned}\right\} \quad \text{for } \Delta\phi_1 \ge 0$$

where we now observe that $(1 - \gamma)(2ab\sigma_e' + 2bl\sigma) = 2ab\sigma_e' + 2bl\sigma - \gamma abl\Delta f$ when $\Delta\phi_1 = 0$; i.e., $\Delta\phi_1 + E_1$ is a continuous

function of l and Δf at the points $(l, \Delta f)$ for which $\Delta\phi_1 = 0$. Note that the greater the value of the apportionment parameter γ, the smaller the value of both $\Delta\phi_1 + E_1$ and E_1.

An expression of l' is not needed in order to evaluate $S_{Total}(T)$ and $\bar{l}(T)$. However, an expression for l' in terms of λ and vice versa will be derived in order to see how l' depends on other quantities in our model. Given $\Delta\phi_1 + E_1 = (1-\lambda)(2ab\sigma_e' + 2bl\sigma)$ for $\Delta\phi_1 < 0$, one can first find ψ *when* $\Delta\phi_1 < 0$ *holds* in terms of λ by equating the expressions

$$(1-\lambda)(2ab\sigma_e' + 2bl\sigma) = 2ab\sigma_e' + 2bl\sigma - \psi abl\Delta f$$

whence

$$\psi = \lambda\left(\frac{2ab\sigma_e' + 2bl\sigma}{abl\Delta f}\right)$$

or

$$\psi = \lambda(2\sigma_e'/l\Delta f + 2\sigma/a\Delta f)$$

Clearly, equating these expressions and expressing ψ when $\Delta\phi_1 < 0$ in terms of λ are valid since decreasing $2ab\sigma_e' + 2bl\sigma$ by an amount $\psi abl\Delta f$ must be equivalent to decreasing $2ab\sigma_e' + 2bl\sigma$ by $\lambda(2ab\sigma_e' + 2bl\sigma)$. Note that the expression $(2\sigma_e'/l\Delta f + 2\sigma/a\Delta f)$ is always less than 1 when $\Delta\phi_1$ is negative. To see this, simply observe that $\Delta\phi_1 < 0$ implies $2ab\sigma_e' + 2bl\sigma < abl\Delta f$ and then divide both sides of this inequality by $abl\Delta f$. But $\psi \equiv l'/l$ for all values of $\Delta\phi_1$ so that

$$l' = \lambda l(2\sigma_e'/l\Delta f + 2\sigma/a\Delta f)$$

Note that since λ cannot exceed 1, the largest possible value of l', i.e., the upper limit on l', is $l(2\sigma_e'/l\Delta f + 2\sigma/a\Delta f)$ for $\Delta\phi_1 < 0$; as mentioned previously, this upper limit is indeed less that l for $\Delta\phi_1 < 0$.

For completeness, one can also find λ *when* $\Delta\phi_1 > 0$ *holds* in terms of ψ by equating the expressions

$$(1-\lambda)(2ab\sigma_e' + 2bl\sigma) = 2ab\sigma_e' + 2bl\sigma - \psi abl\Delta f$$

whence

$$\lambda = \frac{\psi}{(2\sigma_e'/l\Delta f + 2\sigma/a\Delta f)}$$

Clearly, equating these expressions and expressing λ when $\Delta\phi_1 > 0$ in terms of ψ are valid since decreasing $2ab\sigma_e' + 2bl\sigma$ by an amount $\psi abl\Delta f$ must be equivalent to decreasing $2ab\sigma_e' + 2bl\sigma$ by $\lambda(2ab\sigma_e' + 2bl\sigma)$. Here again, $\psi \equiv l'/l$, and $\lambda = (l'/l)(1/(2\sigma_e'/l\Delta f + 2\sigma/a\Delta f))$. Note that $(2\sigma_e'/l\Delta f + 2\sigma/a\Delta f)$ is always greater than 1 when $\Delta\phi_1$ is positive.

In summary, then, for $\Delta\phi_1 \le 0$, one chooses a value from 0 to 1 for the parameter γ, whence $\lambda = \gamma$, and then calculates $\psi = \lambda(2\sigma_e'/l\Delta f + 2\sigma/a\Delta f)$. For $\Delta\phi_1 \ge 0$, one chooses a value from 0 to 1 for the parameter γ, whence $\psi = \gamma$, and then calculates $\lambda = \psi/(2\sigma_e'/l\Delta f + 2\sigma/a\Delta f)$. Thus

$$\left.\begin{aligned}\lambda &= \gamma\\ \psi &= \lambda(2\sigma_e'/l\Delta f + 2\sigma/a\Delta f)\end{aligned}\right\} \text{for } \Delta\phi_1 \le 0$$

$$\left.\begin{aligned}\psi &= \gamma\\ \lambda &= \frac{\psi}{(2\sigma_e'/l\Delta f + 2\sigma/a\Delta f)}\end{aligned}\right\} \text{for } \Delta\phi_1 \ge 0$$

For all $\Delta\phi_1$, one can calculate l' from $l' = \psi l$ or from $l' = \lambda l(2\sigma_e'/l\Delta f + 2\sigma/a\Delta f)$.

Incidentally, the constraint $2ab\sigma_e' + 2bl\sigma - \psi abl\Delta f \ge 0$ combined with $0 \le \psi \le 1$ implies that the inequality

$$0 \le \psi \le \text{the smaller of 1 and } (2\sigma_e'/l\Delta f + 2\sigma/a\Delta f)$$

must be satisfied, and clearly our theory has satisfied it. Similarly, the constraint $abl\Delta f - \lambda(2ab\sigma_e' + 2bl\sigma) \ge 0$ combined with $0 \le \lambda \le 1$ implies that the inequality

$$0 \le \lambda \le \text{the smaller of 1 and } \frac{1}{(2\sigma_e'/l\Delta f + 2\sigma/a\Delta f)}$$

must be satisfied, and clearly our theory has satisfied it.

The approach developed above can readily be applied to incorporate into the model the constraint that E_e be nonnegative. Here, $E_2 = 2ab\sigma_e - \hat{\psi}abl\Delta f$ can be negative when E is positive, and E is always positive (except when $l = 2\sigma_e/\Delta f$, which gives $E = 0$). The requirement $E_2 \ge 0$ implies that one is not allowed to apportion all of the free energy of fusion $abl\Delta f$. If the amount $\hat{\psi}abl\Delta f$ which is apportioned were to exceed $2ab\sigma_e$, then E_2 would be negative. Therefore, one has $E_2 = \eta 2ab\sigma_e$ where η is an apportionment parameter with $0 \le \eta \le 1$. $E + E_2 = -2ab\sigma_e + abl\Delta f + \eta 2ab\sigma_e = abl\Delta f - (1-\eta)2ab\sigma_e$. For convenience, make the change of variable $\theta \equiv 1 - \eta$ with $0 \le \theta \le 1$ so that for all l and Δf

$$E_2 = (1-\theta)(2ab\sigma_e) \quad \text{and} \quad E + E_2 = abl\Delta f - \theta(2ab\sigma_e)$$

Observe that the barrier $E + E_2$ to the destruction of the second and each subsequent stem cannot be smaller than the free energy increase E that occurs upon its destruction, which implies that an adsorbed second or subsequent stem cannot completely crystallize before the barrier to the formation of the stem is surmounted, i.e., that the upper limit, determined below, on l'' is less than l.

To find an expression for l'' in terms of θ, one first finds $\hat{\psi}$ in terms of θ by equating the expressions for E_2; i.e.

$$(1-\theta)(2ab\sigma_e) = 2ab\sigma_e - \hat{\psi}abl\Delta f$$

whence

$$\hat{\psi} = \theta(2\sigma_e/l\Delta f)$$

Clearly, equating these expressions and expressing $\hat{\psi}$ in terms of θ are valid since decreasing $2ab\sigma_e$ by an amount $\hat{\psi}abl\Delta f$ must be equivalent to decreasing $2ab\sigma_e$ by $\theta(2ab\sigma_e)$. Note that the constraint $2ab\sigma_e - \hat{\psi}abl\Delta f \ge 0$ implies that the inequality $0 \le \hat{\psi} \le 2\sigma_e/l\Delta f$ must be satisfied; since $0 \le \theta \le 1$ holds, we have indeed satisfied this inequality. Also note that $2\sigma_e/l\Delta f$ is always less than or equal to 1 since $l \ge 2\sigma_e/\Delta f$ has been established. (Incidentally, $2ab\sigma_e - \hat{\psi}abl\Delta f \ge 0$ does *not* imply constraints $l \le 2\sigma_e/\hat{\psi}\Delta f$, $\Delta f \le 2\sigma_e/\hat{\psi}l$, or $\sigma_e \ge \hat{\psi}l\Delta f/2$.) Finally, recalling that $\hat{\psi} = l''/l$ and substituting above gives $l'' = \theta(2\sigma_e/\Delta f)$.

In the special case $\gamma = \theta = 0$, our model reduces to the case $\psi = \hat{\psi} = 0$ of the LH model which permits negative barriers for nonzero ψ.

VI. Determination of the Sign of $\Delta\phi_1$

At this point, one needs to determine when $\Delta\phi_1$ is positive, zero, and negative. Now $\Delta\phi_1 = 2ab\sigma_e' + 2bl\sigma - abl\Delta f \ge 0$ implies $bl(2\sigma - a\Delta f) \ge -2ab\sigma_e'$; and there are three cases to consider.

Case a: $2\sigma - a\Delta f > 0$ or $\Delta f < 2\sigma/a$. Then the inequality $l > -2ab\sigma_e'/[b(2\sigma - a\Delta f)]$ is always satisfied since l is always greater than zero, and hence $\Delta\phi_1 > 0$ holds.

Case b: $2\sigma - a\Delta f = 0$ or $\Delta f = 2\sigma/a$. Then $\Delta\phi_1 = 2ab\sigma_e'$, which is always positive or zero depending on σ_e'.

Thus, combining cases a and b, we have $\Delta\phi_1 \ge 0$ for all l when $\Delta f \le 2\sigma/a$, where $\Delta\phi_1 = 0$ when both $\sigma_e' = 0$ and $\Delta f = 2\sigma/a$.

Case c: $2\sigma - a\Delta f < 0$ or $\Delta f > 2\sigma/a$. Then $\Delta\phi_1 \geq 0$ implies $-bl(a\Delta f - 2\sigma) \geq -2ab\sigma_e'$ or $l \leq (2\sigma_e'/\Delta f)/(1 - 2\sigma/a\Delta f) \equiv l_0$. Thus, when $\Delta f > 2\sigma/a$, $\Delta\phi_1 \geq 0$ holds for $l \leq l_0$, and $\Delta\phi_1 \leq 0$ holds for $l \geq l_0$. (Observe that as $\Delta f \to 2\sigma/a$ from values greater than $2\sigma/a$, $l_0 \to \infty$.) There is, however, one further condition to consider here. Recall that $l \geq 2\sigma_e/\Delta f$ has been established. If $l_0 < 2\sigma_e/\Delta f$ holds, then $l > l_0$ holds and consequently $\Delta\phi_1 < 0$ would hold for all l. To determine when $l_0 < 2\sigma_e/\Delta f$ holds, simply write $(2\sigma_e'/\Delta f)/(1 - 2\sigma/a\Delta f) < 2\sigma_e/\Delta f$, and noting that $2\sigma/a\Delta f < 1$, rearrange this inequality to get $2\sigma/a\Delta f < (\sigma_e - \sigma_e')/\sigma_e$. Now, if $\sigma_e \leq \sigma_e'$, this inequality would be $2\sigma/a\Delta f < 0$, which is never satisfied; hence, $l_0 < 2\sigma_e/\Delta f$ never occurs when $\sigma_e \leq \sigma_e'$. If $\sigma_e > \sigma_e'$, $l_0 < 2\sigma_e/\Delta f$ occurs when $\Delta f > (2\sigma/a)[\sigma_e/(\sigma_e - \sigma_e')]$. Thus, if $\sigma_e > \sigma_e'$ and $2\sigma/a < \Delta f \leq (2\sigma/a)[\sigma_e/(\sigma_e - \sigma_e')]$, $\Delta\phi_1 \geq 0$ holds for $l \leq l_0$ and $\Delta\phi_1 \leq 0$ holds for $l \geq l_0$, but for $\Delta f > (2\sigma/a)[\sigma_e/(\sigma_e - \sigma_e')]$, $\Delta\phi_1 < 0$ holds for all l.

VII. Expression for $S_{\text{Total}}(T)$ and $\bar{l}(T)$

If $\sigma_e \leq \sigma_e'$, our model with no negative barriers has

(1) $\Delta\phi_1 + E_1 = 2ab\sigma_e' + 2bl\sigma - \gamma abl\Delta f$ for $\Delta f \leq 2\sigma/a$

(2) $\Delta\phi_1 + E_1 = 2ab\sigma_e' + 2bl\sigma - \gamma abl\Delta f$ for $\Delta f > 2\sigma/a$ and $l \leq l_0$

(2) $\Delta\phi_1 + E_1 = (1 - \gamma)(2ab\sigma_e' + 2bl\sigma)$ for $\Delta f > 2\sigma/a$ and $l \geq l_0$

and if $\sigma_e > \sigma_e'$

(1) $\Delta\phi_1 + E_1 = 2ab\sigma_e' + 2bl\sigma - \gamma abl\Delta f$ for $\Delta f \leq 2\sigma/a$

(2) $\Delta\phi_1 + E_1 = 2ab\sigma_e' + 2bl\sigma - \gamma abl\Delta f$ for $2\sigma/a < \Delta f \leq \frac{2\sigma}{a}\left(\frac{\sigma_e}{\sigma_e - \sigma_e'}\right)$ and $l \leq l_0$

(2) $\Delta\phi_1 + E_1 = (1 - \gamma)(2ab\sigma_e' + 2bl\sigma)$ for $2\sigma/a < \Delta f \leq \frac{2\sigma}{a}\left(\frac{\sigma_e}{\sigma_e - \sigma_e'}\right)$ and $l \geq l_0$

(3) $\Delta\phi_1 + E_1 = (1 - \gamma)(2ab\sigma_e' + 2bl\sigma)$ for $\Delta f > \frac{2\sigma}{a}\left(\frac{\sigma_e}{\sigma_e - \sigma_e'}\right)$

The purpose of categories (1)–(3) will be seen shortly.

When $\Delta\phi_1 + E_1 = 2ab\sigma_e' + 2bl\sigma - \gamma abl\Delta f$, $E_1 = (1 - \gamma)abl\Delta f$, which we call case I.

When $\Delta\phi_1 + E_1 = (1 - \gamma)(2ab\sigma_e' + 2bl\sigma)$, $E_1 = abl\Delta f - \gamma(2ab\sigma_e' + 2bl\sigma)$, which we call case II.

One always has

$$E_2 = (1 - \theta)(2ab\sigma_e)$$

$$E + E_2 = -2ab\sigma_e + abl\Delta f + E_2 = abl\Delta f - \theta 2ab\sigma_e$$

Also

$$S(l,T) = \frac{N_0A_0(1 - B/A)}{1 - B/A + B_1/A}$$

where $B/A = e^{-E/kT}$, $B_1/A = e^{-(E_1-E_2)/kT}$, and $A_0 = \beta e^{-(\Delta\phi_1+E_1)/kT}$.

Abbreviate $c' \equiv 2ab\sigma_e'/kT$, $c \equiv 2ab\sigma_e/kT$, and $\alpha \equiv 2\sigma/a\Delta f$, and recall $l_1 = 2\sigma_e/\Delta f$. Then $c/l_1 = ab\Delta f/kT$, $\alpha c/l_1 = 2b\sigma/kT$, and $E/kT = -c + (c/l_1)l$.

For case I

$$\frac{\Delta\phi_1 + E_1}{kT} = \frac{2ab\sigma_e'}{kT} + \frac{2bl\sigma}{kT} - \frac{\gamma abl\Delta f}{kT} = c' + \frac{c}{l_1}(\alpha - \gamma)l$$

$$\frac{E_1 - E_2}{kT} = \frac{(1 - \gamma)abl\Delta f}{kT} - \frac{(1 - \theta)2ab\sigma_e}{kT} = \frac{c}{l_1}(1 - \gamma)l - (1 - \theta)c$$

For case II

$$\frac{\Delta\phi_1 + E_1}{kT} = \frac{(1 - \gamma)(2ab\sigma_e' + 2bl\sigma)}{kT} = (1 - \gamma)c' + \frac{\alpha c}{l_1}(1 - \gamma)l$$

$$\frac{E_1 - E_2}{kT} = \frac{abl\Delta f - \gamma(2ab\sigma_e' + 2bl\sigma)}{kT} - \frac{(1 - \theta)2ab\sigma_e}{kT} = \frac{c}{l_1}(1 - \alpha\gamma)l - \gamma c' - (1 - \theta)c$$

For case I

$$S_I(l,T) = \frac{\beta N_0 e^{-c'} e^{-(\alpha-\gamma)cl/l_1}(1 - e^c e^{-cl/l_1})}{1 - e^c e^{-cl/l_1} + e^{(1-\theta)c} e^{-(1-\gamma)cl/l_1}}$$

For case II

$$S_{II}(l,T) = \frac{\beta N_0 e^{-(1-\gamma)c'} e^{-(1-\gamma)\alpha cl/l_1}(1 - e^c e^{-cl/l_1})}{1 - e^c e^{-cl/l_1} + e^{(1-\theta)c} e^{\gamma c'} e^{-(1-\alpha\gamma)cl/l_1}}$$

For any Δf in category (1), then

$$S_{\text{Total}}^{(1)}(T) = \frac{1}{l_u}\int_{l_1}^{\infty} S_I(l,T)\,dl \quad \text{and}$$

$$\bar{l}^{(1)}(T) = \frac{\int_{l_1}^{\infty} lS_I(l,T)\,dl}{\int_{l_1}^{\infty} S_I(l,T)\,dl}$$

For any Δf in category (2), then

$$S_{\text{Total}}^{(2)}(T) = \frac{1}{l_u}\int_{l_1}^{l_0} S_I(l,T)\,dl + \frac{1}{l_u}\int_{l_0}^{\infty} S_{II}(l,T)\,dl$$

and

$$\bar{l}^{(2)}(T) = \frac{\int_{l_1}^{l_0} lS_I(l,T)\,dl + \int_{l_0}^{\infty} lS_{II}(l,T)\,dl}{\int_{l_1}^{l_0} S_I(l,T)\,dl + \int_{l_0}^{\infty} S_{II}(l,T)\,dl}$$

For any Δf in category (3), then

$$S_{\text{Total}}^{(3)}(T) = \frac{1}{l_u}\int_{l_1}^{\infty} S_{II}(l,T)\,dl \quad \text{and}$$

$$\bar{l}^{(3)}(T) = \frac{\int_{l_1}^{\infty} lS_{II}(l,T)\,dl}{\int_{l_1}^{\infty} S_{II}(l,T)\,dl}$$

For purposes of comparison, the LH model which permits negative barriers has, for all l and Δf

$$\Delta\phi_1 + E_1 = 2ab\sigma_e' + 2bl\sigma - \psi abl\Delta f \quad \text{and} \quad E_2 = 2ab\sigma_e - \hat{\psi}abl\Delta f$$

so that

$$\frac{E_1 - E_2}{kT} = (1 - \psi + \hat{\psi})\frac{c}{l}l - c$$

and

$$S^{(LH)}(l,T) = \frac{\beta N_0 e^{-c'} e^{-(\alpha-\psi)cl/l_1}(1 - e^{c} e^{-cl/l_1})}{1 - e^{c} e^{-cl/l_1} + e^{c} e^{-(1-\psi+\hat{\psi})cl/l_1}}$$

and

$$S^{(LH)}_{Total}(l,T) = \frac{1}{l_u}\int_{l_1}^{\infty} S^{(LH)}(l,T)\, dl \quad \text{and}$$

$$\bar{l}^{(LH)}(T) = \frac{\int_{l_1}^{\infty} l S^{(LH)}(l,T)\, dl}{\int_{l_1}^{\infty} S^{(LH)}(l,T)\, dl}$$

As is the case in the LH model, our model has two parameters. The most logical choice for θ is $\theta = \gamma$; however, even with $\theta = \gamma$, our integrals cannot be evaluated analytically. There seems to be no special case (other than $\theta = \gamma = 0$) for which they could be evaluated analytically. At this point then, we proceed without setting $\theta = \gamma$.

VIII. Evaluation of the $S_{Total}(T)$ and $\bar{l}(T)$, The Variable Transformations for the Numerical Integrations

The required numerical integrations were easily performed interactively on the VAX using the IMSL subroutine DQDAGS.[10] Integrals to be evaluated using DQDAGS cannot have an infinite limit of integration. One way to proceed before using DQDAGS is to make a change of integration variable. Although DQDAGS can integrate functions with end-point singularities (when the end points are finite), a change of variable which results in a transformed integrand, which is bounded at all points including the finite end points in the new range of integration, is preferable to a change of variable which yields an improper integral albeit with finite integration limits. For each of the integrals appearing in $S^{(1)}_{Total}(T)$, $S^{(2)}_{Total}(T)$, and $S^{(3)}_{Total}(T)$, a variable transformation which resulted in a proper integral was in fact found. The same transformations did not transform the corresponding integrals in the numerators of $\bar{l}^{(1)}$, $\bar{l}^{(2)}(T)$, and $\bar{l}^{(3)}(T)$ into proper integrals; however, the transformed integrands were of the form $(-\ln x)f(x)$ with the singularity resulting only from the factor $\ln x$ as $x \to 0$. This end-point singularity could be handled by DQDAGS.

Consider first the integral in $S^{(1)}_{Total}(T)$. The variable transformation consists of defining

$$x \equiv e^{(1-\gamma)c} e^{-(1-\gamma)cl/l_1}$$

Note that $x(l\to\infty) = 0$; the constant $e^{(1-\gamma)c}$, i.e., the l-independent factor, is chosen so that $x(l=l_1) = 1$. Solving for l in terms of x gives $l = l_1[1 - \ln x/(1-\gamma)c]$ provided $\gamma \neq 1$. Then $dl = -l_1/(1-\gamma)c(1/x)\, dx$. Furthermore, $e^{-(\alpha-\gamma)cl/l_1} = e^{-(\alpha-\gamma)c} x^{(\alpha-\gamma)/(1-\gamma)}$, $e^{-cl/l_1} = e^{-c} x^{1/(1-\gamma)}$, and $e^{-(1-\gamma)cl/l_1} = e^{-(1-\gamma)c} x$ so that

$$S^{(1)}_{Total}(T) = \frac{\beta N_0}{l_u}\frac{e^{-c'} e^{-(\alpha-\gamma)c} l_1}{(1-\gamma)c}\int_0^1 \frac{x^{(\alpha-\gamma)/(1-\gamma)}(1 - x^{1/(1-\gamma)})}{1 - x^{1/(1-\gamma)} + e^{(1-\theta)c} e^{-(1-\gamma)c} x}\left(\frac{1}{x}\right) dx$$

Simplying gives

$$S^{(1)}_{Total}(T) = \frac{\beta N_0}{l_u}\frac{e^{-c'} e^{-(\alpha-\gamma)c} l_1}{(1-\gamma)c}\int_0^1 \frac{x^{(\alpha-1)/(1-\gamma)}(1 - x^{1/(1-\gamma)})}{1 - x^{1/(1-\gamma)} + e^{-(\theta-\gamma)c} x}\, dx$$

This is one of the integrals that was evaluated numerically by DQDAGS. Designate the integrand above as $f_1(x)$.

Using the same variable transformation to evaluate the numerator of $\bar{l}^{(1)}(T)$ gives

$$\bar{l}^{(1)}(T) = \frac{\int_0^1 l_1\left[1 - \frac{(\ln x)}{(1-\gamma)c}\right] f_1(x)\, dx}{\int_0^1 f_1(x)\, dx} = l_1 + \frac{l_1}{(1-\gamma)c}\frac{\int_0^1 (-\ln x) f_1(x)\, dx}{\int_0^1 f_1(x)\, dx}$$

Next, using the transformation on the integral $\int_{l_1}^{l_0} S_I(l,T)\, dl$ appearing in $S^{(2)}_{(total)}(T)$ gives

$$\int_{l_1}^{l_0} S_I(l,T)\, dl = \beta N_0 \frac{e^{-c'} e^{-(\alpha-\gamma)c} l_1}{(1-\gamma)c}\int_{x_0}^1 f_1(x)\, dx$$

where

$$x_0 \equiv x(l=l_0) = e^{(1-\gamma)c} e^{-(1-\gamma)cl_0/l_1} = e^{(1-\gamma)c} e^{-(1-\gamma)c'/(1-\alpha)}$$

with $l_0 \equiv 2\sigma_e'/(1-\alpha)\Delta f$ as defined previously. Similarly, the integral $\int_{l_1}^{l_0} l S_I(l,T)\, dl$ appearing in $\bar{l}^{(2)}(T)$ becomes

$$\int_{l_1}^{l_0} l S_I(l,T)\, dl = \frac{\beta N_0 e^{-c'} e^{-(\alpha-\gamma)c} l_1}{(1-\gamma)c}\left\{l_1\int_{x_0}^1 f_1(x)\, dx + \frac{l_1}{(1-\gamma)c}\int_{x_0}^1 (-\ln x) f_1(x)\, dx\right\}$$

A different transformation is made on the integral $\int_{l_0}^{\infty} S_{II}(l,T)\, dl$ also appearing in $S^{(2)}_{Total}(T)$. Here, define

$$x \equiv e^{(1-\gamma)(c-c')} e^{-(1-\gamma)\alpha cl/l_1}$$

Again $x(l\to\infty) = 0$; the constant $e^{(1-\gamma)(c-c')}$ is chosen so that $x(l=l_0) = x_0$, which is given above. Solving for l gives $l = (l_1/\alpha c)[c - c' - (\ln x)/(1-\gamma)]$ provided $\gamma \neq 1$. Then $dl = -l_1/(1-\gamma)\alpha c(1/x)\, dx$. Furthermore, $e^{-(1-\gamma)\alpha cl/l_1} = e^{-(1-\gamma)(c-c')} x$, $e^{-cl/l_1} = e^{-(c-c')/\alpha} x^{1/(1-\gamma)\alpha}$, and $e^{-(1-\alpha\gamma)cl/l_1} = e^{-(c-c')(1-\alpha\gamma)/\alpha} x^{(1-\alpha\gamma)/(1-\gamma)\alpha}$. Substituting gives

$$\int_{l_0}^{\infty} S_{II}(l,T)\, dl = \frac{\beta N_0 e^{-(1-\gamma)c'} e^{-(1-\gamma)(c-c')} l_1}{(1-\gamma)\alpha c} \times \int_0^{x_0} x(1 - e^{c} e^{-((c-c')/\alpha)} x^{1/(1-\gamma)\alpha})\left(\frac{1}{x}\right) dx/[1 - e^{c} e^{-((c-c')/\alpha)} x^{1/(1-\gamma)\alpha} + e^{(1-\theta)c} e^{\gamma c'} e^{-((c-c')/\alpha)(1-\alpha\gamma)} x^{(1-\alpha\gamma)/(1-\gamma)\alpha}] =$$

$$\frac{\beta N_0 e^{-(1-\gamma)c} l_1}{(1-\gamma)\alpha c}\int_0^{x_0} 1 - e^{c} e^{-(c-c'/\alpha)} x^{1/(1-\gamma)\alpha}\, dx/ [1 - e^{c} e^{-((c-c')/\alpha)} x^{1/(1-\gamma)\alpha} + e^{-(\theta-\gamma)c} e^{c} e^{-((c-c')/\alpha)} x^{(1-\alpha\gamma)/(1-\gamma)\alpha}]$$

Designate the integrand above as $f_2(x)$. Similarly, the integral $\int_{l_0}^{\infty} l S_{II}(l,T)\, dl$ appearing in $\bar{l}^{(2)}(T)$ becomes

$$\int_{l_0}^{\infty} l S_{II}(l,T)\, dl = \frac{\beta N_0 e^{-(1-\gamma)c} l_1}{(1-\gamma)\alpha c}\left\{\frac{(c-c')}{\alpha c} l_1 \int_0^{x_0} f_2(x)\, dx + \frac{l_1}{(1-\gamma)\alpha c}\int_0^{x_0} (-\ln x) f_2(x)\, dx\right\}$$

Thus

$$S^{(2)}_{Total}(T) = \left(\frac{\beta N_0}{l_u}\frac{e^{-c'} e^{-(\alpha-\gamma)c} l_1}{(1-\gamma)c}\int_{x_0}^1 f_1(x)\, dx\right) + \left(\frac{\beta N_0}{l_u}\frac{e^{-(1-\gamma)c} l_1}{(1-\gamma)\alpha c}\int_0^{x_0} f_2(x)\, dx\right)$$

and

$$\bar{l}^{(2)}(T) = \frac{\left(\frac{1}{\beta N_0}\int_{l_1}^{l_0} lS_{\mathrm{I}}(l,T)\,\mathrm{d}l\right) + \left(\frac{1}{\beta N_0}\int_{l_0}^{\infty} lS_{\mathrm{II}}(l,T)\,\mathrm{d}l\right)}{\frac{l_{\mathrm{u}}}{\beta N_0}S^{(2)}_{\mathrm{Total}}(T)}$$

with the appropriate expressions for the integrals and $S^{(2)}_{\mathrm{Total}}(T)$ to be substituted above.

Finally, consider the integral in $S^{(3)}_{\mathrm{Total}}(T)$. The variable transformation to be made on this integral is

$$x \equiv e^{(1-\gamma)\alpha c} e^{-(1-\gamma)\alpha c l/l_1}$$

Again $x(l\to\infty) = 0$ and the constant $e^{(1-\gamma)\alpha c}$ is chosen so that $x(l=l_1) = 1$. Solving for l gives $l = l_1[1 - (\ln x)/(1-\gamma)\alpha c]$ provided $\gamma \neq 1$. Then $\mathrm{d}l = -[l_1/(1-\gamma)\alpha c](1/x)\,\mathrm{d}x$. Furthermore, $e^{-(1-\gamma)\alpha c l/l_1} = e^{-(1-\gamma)\alpha c}x$, $e^{-cl/l_1} = e^{-c}x^{1/(1-\gamma)\alpha}$, and $e^{-(1-\alpha\gamma)cl/l_1} = e^{-(1-\alpha\gamma)c}x^{(1-\alpha\gamma)/(1-\gamma)\alpha}$ so that

$$S^{(3)}_{\mathrm{Total}}(T) = \frac{\beta N_0}{l_{\mathrm{u}}}\frac{e^{-(1-\gamma)(c'+\alpha c)l_1}}{(1-\gamma)\alpha c}\times \int_0^1 \frac{(1-x^{1/(1-\gamma)\alpha})}{1-x^{1/(1-\gamma)\alpha} + e^{-\theta c}e^{\gamma(c'+\alpha c)}x^{(1-\alpha\gamma)/(1-\gamma)\alpha}}\,\mathrm{d}x$$

Designate the integrand above as $f_3(x)$. Using the same transformation to evaluate the numerator of $\bar{l}^{(3)}(T)$ gives

$$\bar{l}^{(3)}(T) = l_1 + \frac{l_1}{(1-\gamma)\alpha c}\frac{\int_0^1(-\ln x)f_3(x)\,\mathrm{d}x}{\int_0^1 f_3(x)\,\mathrm{d}x}$$

IX. Results and Discussion

A VAX FORTRAN program was written to evaluate the required mathematical expressions. All calculations were done with double precision using the model parameter values given in Figure 3 of ref 4; namely, $a = b = 5\times10^{-8}$ cm, $\sigma = 10$ erg/cm^2, $\sigma_e = 100$ erg/cm^2, $T_m^\circ = 500$ K, $\Delta h = 3\times10^9$ ergs/cm^3, and $\Delta f = (T_m^\circ - T)\Delta h/T_m^\circ$, where Δh is the enthalpy of fusion at $T = T_m^\circ$. The average lamellar thickness calculated from the LH model is independent of σ_e'; this is true for our model only for $\Delta f \le 2\sigma/a$, however. Other quantities such as $S_{\mathrm{Total}}(T)$ do depend on σ_e' even in the LH model, and physically,[11] one expects $0 \le \sigma_e' \le \sigma_e$. In the case $\sigma_e' \equiv 0$, our model is slightly simpler, for then

$$\left.\begin{aligned}\Delta\phi_1 + E_1 &= 2bl\sigma - \gamma abl\Delta f\\ E_1 &= (1-\gamma)abl\Delta f\end{aligned}\right\} \quad \Delta f \le 2\sigma/a$$

$$\left.\begin{aligned}\Delta\phi_1 + E_1 &= (1-\gamma)2bl\sigma\\ E_1 &= abl\Delta f - \gamma 2bl\sigma\end{aligned}\right\} \quad \Delta\phi > 2\sigma/a$$

Let us investigate our model in detail for the case $\sigma_e' = 0$ first; this is also the somewhat arbitrary choice for σ_e' made for the calculations[1,2] for the LH model. For the values of a, σ, T_m°, and Δh given above, the temperature T^* for which $\Delta f = 2\sigma/a$ is $T^* = 433\,^1/_3$ K.

Given the parameter values above and now with the choice $\theta = \gamma$, the calculated average lamellar thickness vs temperature curves ($\bar{l}$ vs T) are plotted in Figure 1a for the selected values of $\gamma = 0$, $^1/_4$, and $^1/_2$. (Results for $\gamma > ^1/_2$ will be discussed later.) Some of the data used to construct these plots are given in Table I. (For $\Delta f \le 2\sigma/a$, the average lamellar thickness is given by the expression for $\bar{l}^{(1)}(T)$ given previously, and, for $\Delta f > 2\sigma/a$, it is given by the expression for $\bar{l}^{(3)}(T)$ also given previously.) Clearly, $\bar{l}$ decreases monotonically with decreasing T in agreement with typical experimental behavior. For most supercoolings, the magnitude of the $\bar{l}$ values is on the order of 25–125 Å, which is quite reasonable. Note that, at least for all values of $\Delta f > 2\sigma/a$, $\bar{l}$ at a given T increases with increasing γ. Also, the numerical results shown in Figure 1a indicate that $\bar{l}$ vs T is relatively insensitive to the value of γ.

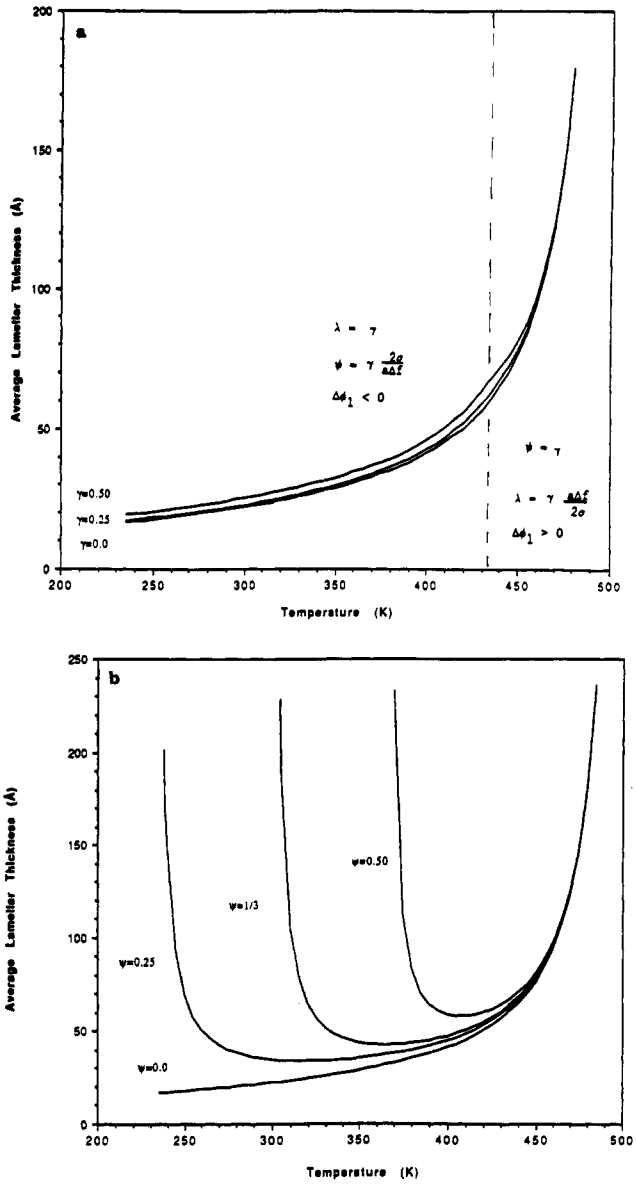

Figure 1. (a) Plots of average lamellar thickness (Å) vs temperature (K) for $\gamma = 0$, $^1/_4$, and $^1/_2$, each with $\sigma_e' = 0$ and $\theta = \gamma$. See section IX for a, b, σ, σ_e, T_m°, and Δh which are the same for all of the figures. At $T = 433\,^1/_3$ K (i.e., $= 2\sigma/a$), $\Delta\phi_1 = 0$. For $T \ge 433\,^1/_3$ K, $\Delta\phi_1 \ge 0$ and $\psi = \gamma$ and $\lambda = \gamma(a\Delta f/2\sigma)$. For $T \le 433\,^1/_3$ K, $\Delta\phi_1 \le 0$ and $\psi = \gamma(2\sigma/a\Delta f)$ and $\lambda = \gamma$. (b) Plots of average lamellar thickness (Å) vs temperature (K) for $\psi = 0$, $^1/_4$, $^1/_3$, and $^1/_2$, each with $\hat{\psi} = \psi$, reproduced from the Lauritzen–Hoffman Model.[1] Plots are independent of σ_e'.

For comparison, we have reproduced part of Figure 3b of ref 1 as our Figure 1b, which shows the LH model $\bar{l}$ vs T curves with $\hat{\psi} = \psi$ for the selected values of $\psi = 0$, $^1/_4$, $^1/_3$, and $^1/_2$. Some of the data which we calculated in order to construct these plots are given in Table II. The LH model $\psi = 0$ curve is identical to our $\gamma = 0$ curve. For $\Delta f \le 2\sigma/a$, each of the LH model "ψ curves" is qualitatively similar but not quantitatively identical to its corresponding "γ curve" presented in Figure 1a. Recall that the quantitative difference arises from the fact that the barrier E_2

Table I
Average Lamellar Thickness (Å) as a Function of Temperature (K) for $\gamma = 0$ and for $\gamma = 1/2$, Each with $\sigma_e' = 0$ and $\theta = \gamma$[a]

temp (K)	$\psi = \gamma = 0$	$\gamma = 1/2$	temp (K)	$\psi = \gamma = 0$	$\gamma = 1/2$
485.000	234.383	235.303	355.000	29.433	33.176
480.000	178.390	179.781	350.000	28.540	32.225
475.000	144.660	146.556	345.000	27.700	31.329
470.000	122.074	124.507	340.000	26.907	30.484
465.000	105.867	108.867	335.000	26.157	29.683
460.000	93.652	97.253	330.000	25.446	28.924
455.000	84.105	88.342	325.000	24.772	28.201
450.000	76.429	81.344	320.000	24.130	27.513
445.000	70.115	75.762	315.000	23.518	26.855
440.000	64.826	71.267	310.000	22.935	26.226
435.000	60.328	67.641	305.000	22.377	25.624
430.000	56.451	63.528	300.000	21.843	25.045
425.000	53.072	59.481	295.000	21.332	24.489
420.000	50.100	55.988	290.000	20.841	23.953
415.000	47.463	52.941	285.000	20.369	23.437
410.000	45.105	50.259	280.000	19.915	22.938
405.000	42.984	47.877	275.000	19.479	22.456
400.000	41.064	45.744	270.000	19.057	21.990
395.000	39.316	43.821	265.000	18.651	21.537
390.000	37.718	42.077	260.000	18.258	21.099
385.000	36.251	40.484	255.000	17.878	20.673
380.000	34.897	39.023	250.000	17.511	20.259
375.000	33.644	37.676	245.000	17.155	19.856
370.000	32.480	36.429	240.000	16.809	19.463
365.000	31.396	35.270	235.000	16.475	19.081
360.000	30.382	34.188			

[a] See Figure 1a. See section IX for a, b, σ, σ_e, $T_m°$, and Δh, which are the same for all of the tables.

has been constrained to be nonnegative; i.e., $E_2 = (1 - \theta)2ab\sigma_e$. For $\Delta f > 2\sigma/a$, however, the LH model ψ curves are in marked contrast to the γ curves; in particular, for each ψ curve, $\bar{l}$ approaches infinity asymptotically as Δf approaches $2\sigma/\psi a$. This is the behavior which is known as the Δl catastrophe.

One point is worth emphasizing here, namely, the relationship between γ and ψ. In both our model and the LH model, $\psi \equiv l'/l$, but this ratio in the LH model is a constant, whereas in our model

$$\psi = \begin{cases} \gamma\left(\dfrac{2\sigma_e'}{l\Delta f} + \dfrac{2\sigma}{a\Delta f}\right) & \Delta\phi_1 \le 0 \\ \gamma & \Delta\phi_1 \ge 0 \end{cases}$$

For the case $\sigma_e' = 0$, this becomes

$$\psi = \begin{cases} \gamma\,\dfrac{2\sigma}{a\Delta f} & \Delta f \ge 2\sigma/a \\ \gamma & \Delta f \le 2\sigma/a \end{cases}$$

Now, for any given ψ, say ψ_j, $\bar{l}$ in the LH model is infinite for all $\Delta f \ge 2\sigma/\psi_j a$; and for all $\Delta f \ge 2\sigma/\psi_j a$, there is no finite value of $\bar{l}$ for any $\psi \ge \psi_j$. Equivalently, a value of $\psi \ge \psi_j$ is not possible for a chain-folded system for all $\Delta f \ge 2\sigma/\psi_j a$; that is, high values of ψ do not lead to chain-folded polymer crystals at high enough supercooling according to the LH model. Experiment, however, gives chain-folded crystals at high supercooling with an average lamellar thickness that decreases monotonically with decreasing temperature. As we have seen, our one-parameter (i.e., γ) model with $\sigma_e' = 0$ does reproduce this high-supercooling behavior. Yet, high values of ψ, i.e., of the ratio l'/l, are *not* associated with our high-supercooling, chain-folded

Table II
Average Lamellar Thickness (Å) as a Function of Temperature (K) for $\psi = 1/2$ with $\hat{\psi} = \psi$, Reproduced from the Lauritzen-Hoffman (LH) Model[4,a]

temp (K)	LH $\psi = 1/2$	temp (K)	LH $\psi = 1/2$	temp (K)	LH $\psi = 1/2$
485.000	235.785	440.000	70.789	400.000	58.577
480.000	180.224	435.000	67.037	395.000	60.458
475.000	146.926	430.000	64.009	390.000	64.019
470.000	124.780	425.000	61.610	385.000	70.494
465.000	109.027	420.000	59.786	380.000	82.999
460.000	97.290	415.000	58.519	375.000	112.171
455.000	88.251	410.000	57.832	370.000	232.547
450.000	81.124	405.000	57.800	365.000	∞
445.000	75.412				

[a] Data are independent of σ_e'. See Figure 1b.

systems. To see this, first introduce the dimensionless quantity x, where $0 < x < 1$. Then for any $\Delta f = 2\sigma/xa$, $\psi = \gamma(2\sigma/a\Delta f) = \gamma x$. Since γ cannot exceed 1, ψ in our model cannot exceed x_j for any $\Delta f \ge 2\sigma/x_j a$, where x_j is any given value of x. But this is exactly what was found for ψ in the LH model, i.e., that a value of ψ greater than or equal to ψ_j is not possible for any $\Delta f \ge 2\sigma/\psi_j a$. Thus, for $\Delta f > 2\sigma/a$, our model, through the imposition of the constraint that barriers be nonnegative, places exactly the same upper limit, $2\sigma/a\Delta f$, on our ψ that is predicted for ψ in the LH model. However, for $\Delta f > 2\sigma/a$, our model, unlike the LH model, predicts $\bar{l}$ vs T in qualitative agreement with experiment.

Thus, the selected calculations done for our model indicate that, for the case $\sigma_e' = 0$, our model does *not* exhibit an infinite average lamellar thickness. Most importantly, our model predicts $\bar{l}$ vs T curves which are monotonically decreasing with decreasing T in agreement with experiment. That is, we have successfully extended the LH model to higher supercooling. Also, this success, coupled with the numerical results shown in Figure 1a, significantly increases our confidence in using $\gamma = 0$ as a first approximation for mathematical convenience in practice.[7] Finally, our results show that the Δl catastrophe of the LH theory is related to the failure to exclude negative barriers and moreover that the LH approach to polymer crystallization is in itself valid for high supercooling—given that negative barriers are forbidden. Prior to this work, the LH approach had always been described as one which is invalid at high supercooling.

One set of results with $\theta \neq \gamma$ is presented in Table III. Here we see that, for $\gamma = 1/2$ and $\theta = 1$, the calculated $\bar{l}(T)$ differ only slightly from the case with $\gamma = 1/2$ and $\theta = 1/2$.

Next, we investigated our model for $\sigma_e' \neq 0$. (Recall that $\bar{l}$ for the LH model is independent of σ_e' and that our model is independent of σ_e' for $\Delta f \le 2\sigma/a$.) Using the same values for a, b, σ, σ_e, $T_m°$, and Δh as above and again with $\theta = \gamma$, $\bar{l}$ vs T curves for $\sigma_e' = 0$, 60, 100, and 150 erg/cm^2—each with $\gamma = 1/2$—are plotted together in Figure 2. Some of the $\sigma_e' \neq 0$ data used to construct these plots are given in Table IV (and the $\sigma_e' = 0$ data has been seen previously in Table I). From Figure 2, we see that $\bar{l}$ decreases monotonically with decreasing T for $0 < \sigma_e' \le \sigma_e$ as well as for $\sigma_e' = 0$ and that $\bar{l}$ vs T is relatively insensitive to the value of $\sigma_e' \le \sigma_e$. Thus our conclusions made immediately above for the case $\sigma_e' = 0$ are valid when $0 \le \sigma_e' \le \sigma_e$. For $\sigma_e' = 150$ erg/cm^2, there is a relative minimum in $\bar{l}$ vs T near $T = 405$ K, and the curve passes through a small and "diffuse" relative maximum at a lower temperature. Recall that one expects $0 \le \sigma_e' \le \sigma_e$ so that, with $\sigma_e = 100$ erg/cm^2, $\sigma_e' = 150$ erg/cm^2 may not be realistic

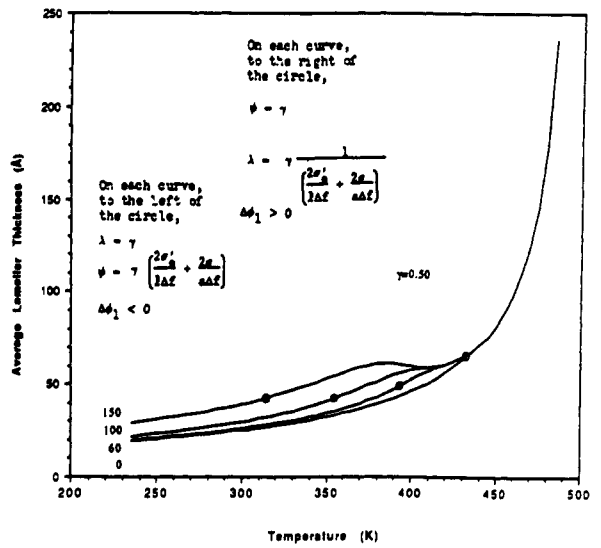

Figure 2. Plots of average lamellar thickness (Å) vs temperature (K) for $\sigma_e' = 0$, 60, 100, and 150 ergs/cm^2, each with $\theta = \gamma = 1/2$. Each oepn circle designates the point $(\bar{l}_0, T_0)$ at which $\Delta\phi_1(\bar{l},T) = 0$. For $T \geq T_0$, $\Delta\phi_1 \geq 0$, $\psi = \gamma$, and $\lambda = \gamma(ab\bar{l}\Delta f/(2ab\sigma_e' + 2b\bar{l}\sigma)$. For $T \leq T_0$, $\Delta\phi_1 \leq 0$, $\psi = \gamma(2\sigma_e'/\bar{l}\Delta f + 2\sigma/a\Delta f)$, and $\lambda = \gamma$.

Table III
Average Lamellar Thickness (Å) as a Function of Temperature (K) for $\gamma = 1/2$, $\theta = 1$, and $\sigma_e' = 0$

temp (K)	$\theta = 1$, $\gamma = 1/2$	temp (K)	$\theta = 1$, $\gamma = 1/2$	temp (K)	$\theta = 1$, $\gamma = 1/2$
495.000	675.848	405.000	46.332	315.000	26.716
490.000		400.000		310.000	
485.000	230.877	395.000	42.690	305.000	25.516
480.000		390.000		300.000	
475.000	142.184	385.000	39.639	295.000	24.405
470.000		380.000		290.000	
465.000	104.542	375.000	37.036	285.000	23.373
460.000		370.000		280.000	
455.000	84.037	365.000	34.779	275.000	22.407
450.000		360.000		270.000	
445.000	71.460	355.000	32.796	265.000	21.501
440.000		350.000		260.000	
435.000	63.333	345.000	31.035	255.000	20.646
430.000		340.000		250.000	
425.000	56.368	335.000	29.454	245.000	19.836
420.000		330.000		240.000	
415.000	50.779	325.000	28.022	235.000	19.067
410.000		320.000			

but is examined in order to explore the model predictions as a function of σ_e'.

The relationship between γ and ψ with $\sigma_e' \neq 0$ is worth emphasing at this point. In doing so, one difference between the cases $\sigma_e' = 0$ and $\sigma_e' \neq 0$ will be found; namely, ψ can exceed ψ_j for some $\Delta f \geq 2\sigma/\psi_j a$ when $\sigma_e' \neq 0$. To reiterate, in both our model and the LH model, $\psi \equiv l'/l$, but this ratio in the LH model is a constant, whereas in our model

$$\psi(l,T) = \begin{cases} \gamma\left(\dfrac{2\sigma_e'}{l\Delta f} + \dfrac{2\sigma}{a\Delta f}\right) & \Delta\phi_1(l,T) \leq 0 \\ \gamma & \Delta\phi_1(l,T) \geq 0 \end{cases}$$

where the notations $\psi(l,T)$ and $\Delta\phi_1(l,T)$ emphasize here the dependence of ψ and $\Delta\phi_1$ and l and T. (The T dependence, of course, enters through Δf.) Recalling the conditions which govern the sign of $\Delta\phi_1$ then gives, when $\sigma_e > \sigma_e'$

$$\psi(l,T) = \begin{cases} \gamma\left(\dfrac{2\sigma_e'}{l\Delta f} + \dfrac{2\sigma}{a\Delta f}\right) & \begin{cases} \text{for all } l \text{ when } \Delta f > \dfrac{2\sigma}{a}\left(\dfrac{\sigma_e}{\sigma_e - \sigma_e'}\right) \\ \text{for } l \geq l_0 \text{ when } \dfrac{2\sigma}{a} < \Delta f \leq \dfrac{2\sigma}{a}\left(\dfrac{\sigma_e}{\sigma_e - \sigma_e'}\right) \end{cases} \\ \gamma & \begin{cases} \text{for } l \geq l_0 \text{ when } \dfrac{2\sigma}{a} < \Delta f \leq \dfrac{2\sigma}{a}\left(\dfrac{\sigma_e}{\sigma_e - \sigma_e'}\right) \\ \text{for all } l \text{ when } \Delta f \leq \dfrac{2\sigma}{a} \end{cases} \end{cases}$$

and when $\sigma_e \leq \sigma_e'$

$$\psi(l,T) = \begin{cases} \gamma\left(\dfrac{2\sigma_e'}{l\Delta f} + \dfrac{2\sigma}{a\Delta f}\right) & \text{for } l \geq l_0 \text{ when } \Delta f > 2\sigma/a \\ \gamma & \begin{cases} \text{for } l \leq l_0 \text{ when } \Delta f > 2\sigma/a \\ \text{for all } l \text{ when } \Delta f \leq 2\sigma/a \end{cases} \end{cases}$$

where $l_0 = (2\sigma_e'/\Delta f)/(1 - 2\sigma/a\Delta f)$. Furthermore, on an $\bar{l}$ vs T curve, one has

$$\psi(\bar{l},T) = \begin{cases} \gamma\left(\dfrac{2\sigma_e'}{\bar{l}\Delta f} + \dfrac{2\sigma}{a\Delta f}\right) & \Delta\phi_1(\bar{l},T) \leq 0 \\ \gamma & \Delta\phi_1(\bar{l},T) \geq 0 \end{cases}$$

where the conditions which govern the sign of $\Delta\phi_1(\bar{l},T)$ are those given above for $\Delta\phi_1(l,T)$ but with l replaced by $\bar{l}$. Therefore, the temperature T_0 of a point $(\bar{l}_0, T_0)$ on an $\bar{l}$ vs T curve and at which $\Delta\phi_1(\bar{l},T) = \Delta\phi_1(\bar{l}_0,T_0) = 0$ is the solution to the following nonlinear algebraic equation in the one unknown T

$$\bar{l}^{(2)}(T) = l_0$$

or

$$\frac{\int_{l_1}^{l_0} lS_I\,dl + \int_{l_0}^{\infty} lS_{II}\,dl}{\int_{l_1}^{l_0} S_I\,dl + \int_{l_0}^{\infty} S_{II}\,dl} = \frac{2\sigma_e'/\Delta f}{1 - 2\sigma/a\Delta f}$$

If $\sigma_e > \sigma_e'$, T_0 will correspond to a value of Δf in the range $2\sigma/a < \Delta f \leq (2\sigma/a)(\sigma_e/(\sigma_e - \sigma_e'))$, but if $\sigma_e \leq \sigma_e'$, T_0 will correspond to a value of Δf in the range $\Delta f > 2\sigma/a$.

Rather than attempt to solve the above equation iteratively, one simply plots the left-hand side $\bar{l}^{(2)}(T)$ vs T and the right-hand side $l_0(T)$ vs T on the same graph, and T_0 is given by a point of intersection of the two curves. Note that, as Δf approaches $2\sigma/a$ from values greater than $2\sigma/a$, l_0 approaches infinity and that l_0 decreases monotonically with decreasing T for $\Delta f > 2\sigma/a$. For each of the $\bar{l}$ vs T curves with $\sigma_e' \neq 0$, we found one point of intersection $(\bar{l}_0, T_0)$, which is designated on each curve by an open circle. We also found that $\bar{l}^{(2)}(T) > \bar{l}_0$ holds when $T < T_0$ and that $\bar{l}^{(2)}(T) < \bar{l}_0$ holds when $T > T_0$. Thus, $\Delta\phi(\bar{l},T) < 0$ holds for $T < T_0$ and $\Delta\phi(\bar{l},T) > 0$ holds for $T > T_0$. Our

Table IV
Average Lamellar Thickness (Å) as a Function of Temperature (K) for σ_e' = 60, 100, and 150 ergs/cm², Each with $\theta = \gamma = 1/2$ (See Figure 2)

temp (K)	σ_e' = 60	σ_e' = 100	σ_e' = 150
485.000	235.303	235.303	235.303
480.000	179.781	179.781	179.781
475.000	146.556	146.556	146.556
470.000	124.507	124.507	124.507
465.000	108.867	108.867	108.867
460.000	97.253	97.253	97.253
455.000	88.342	88.342	88.342
450.000	81.344	81.344	81.344
445.000	75.762	75.762	75.762
440.000	71.267	71.267	71.267
435.000	67.641	67.641	67.641
430.000	64.735	64.735	64.735
425.000	62.454	62.454	62.454
420.000	60.723	60.743	60.743
415.000	59.214	59.577	59.584
410.000	57.306	58.874	59.005
405.000	54.856	58.337	58.984
400.000	52.149	57.582	59.533
395.000	49.469	56.411	60.296
390.000	46.971	54.852	60.919
385.000	44.708	53.035	61.120
380.000	42.683	51.095	60.800
375.000	40.874	49.136	60.003
370.000	39.252	47.220	58.842
365.000	37.791	45.385	57.434
360.000	36.466	43.648	55.882
355.000	35.253	42.015	54.261
350.000	34.136	40.486	52.625
345.000	33.100	39.056	51.009
340.000	32.131	37.719	49.436
335.000	31.219	36.468	47.918
330.000	30.358	35.295	46.462
325.000	29.541	34.194	45.072
320.000	28.766	33.159	43.746
315.000	28.028	32.183	42.485
310.000	27.324	31.262	41.286
305.000	26.652	30.390	40.145
300.000	26.009	29.564	39.059
295.000	25.392	28.778	38.025
290.000	24.799	28.031	37.040
285.000	24.229	27.318	36.101
280.000	23.681	26.637	35.204
275.000	23.152	25.985	34.346
270.000	22.641	25.360	33.526
265.000	22.147	24.760	32.740
260.000	21.669	24.184	31.986
255.000	21.206	23.628	31.263
250.000	20.756	23.093	30.567
245.000	20.320	22.576	29.898
240.000	19.896	22.076	29.253
235.000	19.484	21.593	28.631

final result is that, on an $\bar{l}$ vs T curve

$$\psi = \begin{cases} \gamma\left(\dfrac{2\sigma_e'}{\bar{l}\Delta f} + \dfrac{2\sigma}{a\Delta f}\right) & 0 < T \le T_0 \\ \gamma & T_0 \le T < T_m^\circ \end{cases}$$

Note that if the dimensionless quantity x, $0 < x < 1$, is again introduced by writing $\Delta f = 2\sigma/xa$, then $\psi = \gamma x((a\sigma_e'/\bar{l}\sigma) + 1)$ so that, unlike the case $\sigma_e' = 0$, ψ can exceed x_j for some $\Delta f \ge 2\sigma/x_j a$, where x_j is any given value of x.

Now, upon proceeding to consider results for $\gamma > 1/2$, our basic conclusions—especially the fact that we have removed the Δl catastrophe at high supercooling—remain intact; however, we do *not* obtain $\bar{l}$ vs T curves which are monotonically decreasing for *all* T when γ is "sufficiently" large. Using the same values for a, b, σ, σ_e, T_m°, and Δh as previously and again with $\theta = \gamma$ and $\sigma_e' = 0$, the calculated

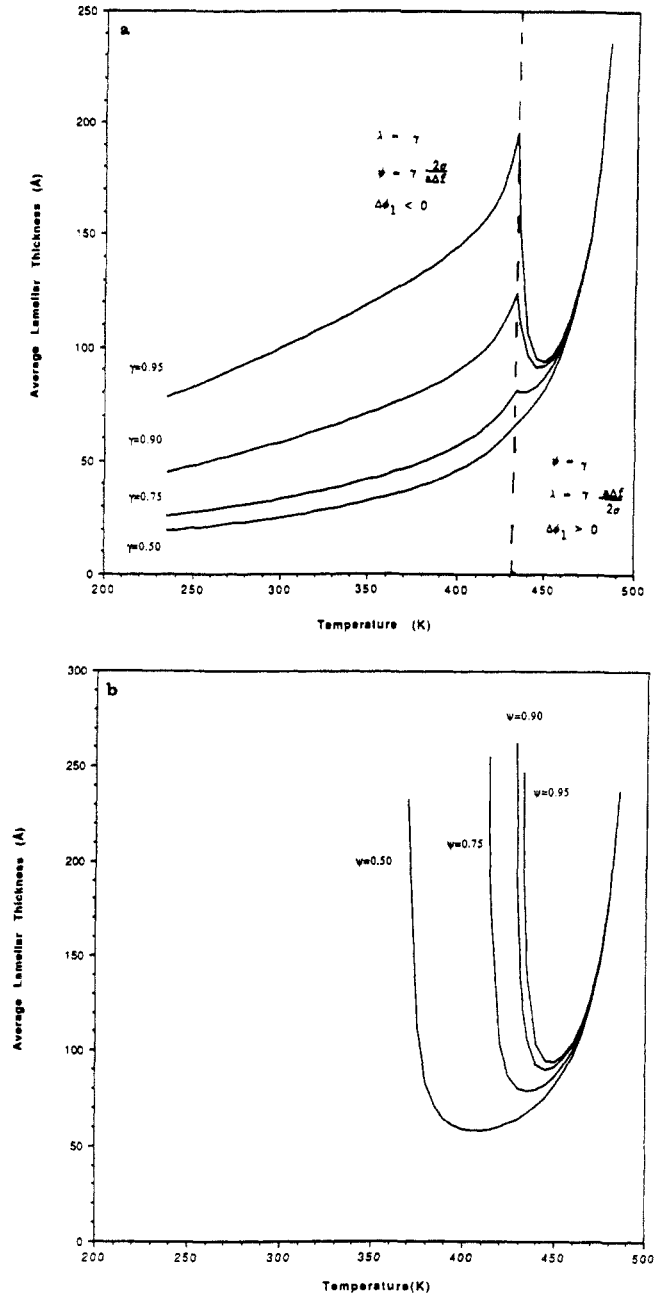

Figure 3. Plots of average lamellar thickness (Å) vs temperature (K) for $\gamma = 1/2, 3/4, 0.90$, and 0.95, each with $\sigma_e' = 0$ and $\theta = \gamma$. As in Figure 1a, $\Delta\phi_1 = 0$ at $T = 433\,1/3$ K. (b) Plots of average lamellar thickness (Å) vs temperature (K) for $\psi = 1/2, 3/4, 0.90$, and 0.95, each with $\hat{\psi} = \psi$, reproduced from the Lauritzen–Hoffman model.[1] Plots are independent of σ_e'.

$\bar{l}$ vs T curves for the selected values of $\gamma = 1/2, 3/4, 0.90$, and 0.95 are plotted in Figure 3a, and the curve for $\gamma = 0.99$ appears in Figure 4. Some of the data used to construct these plots are given in Table V. The effect of γ on $\bar{l}$ as a function of T is readily apparent. First, the curve for $\gamma = 1/2$ appears, on closer examination, to exhibit a discontinuity or break in its slope at the temperature T^* = 433(1/3) K for which $\Delta f = 2\sigma/a$. (This statement will be qualified later.) As for $\gamma = 1/2$, $\bar{l}$ for $\gamma = 3/4$, 0.9, 0.95, and 0.99 does decrease with decreasing T for all T for which $\Delta f > 2\sigma/a$, and there appears to be a break in the slope of $\bar{l}$ vs T at $T = T^*$. Unlike for $\gamma = 1/2$, the higher γ curves pass through a relative minimum at a temperature for which $\Delta f < 2\sigma/a$; the temperature T_* at which this minimum occurs increases with γ (for $\gamma = 3/4$, it occurs between T = 440 and 433 1/3 K and so can hardly be seen on the plot). Also, over the interval $T < T_*$, $\bar{l}$ vs T is at

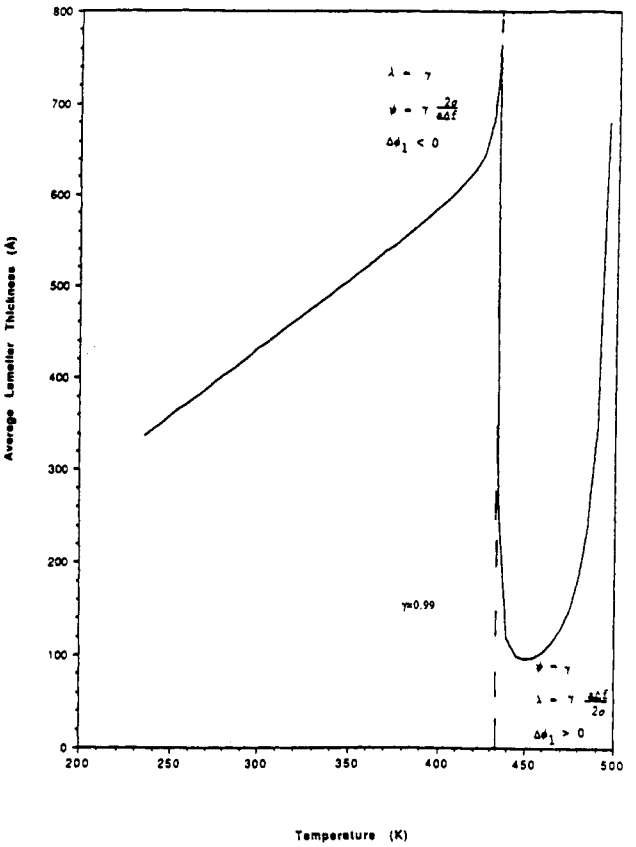

Figure 4. Plots of average lamellar thickness (Å) vs temperature (K) for $\theta = \gamma = 0.99$ and $\sigma_e' = 0$. As in Figure 1a, $\Delta\phi_1 = 0$ at $T = 433^1/_3$ K.

Table V
Average Lamellar Thickness (Å) as a Function of Temperature (K) for $\gamma = 0.90$ with $\sigma_e' = 0$ and $\theta = \gamma$ (See Figure 3a)

temp (K)	$\gamma = 0.90$	temp (K)	$\gamma = 0.90$	temp (K)	$\gamma = 0.90$
485.000	236.013	400.000	89.529	315.000	61.519
480.000	180.939	395.000	86.992	310.000	60.352
475.000	148.300	390.000	84.676	305.000	59.210
470.000	127.027	385.000	82.538	300.000	58.090
465.000	112.435	380.000	80.545	295.000	56.992
460.000	102.279	375.000	78.673	290.000	55.913
455.000	95.475	370.000	76.905	285.000	54.853
450.000	91.672	365.000	75.225	280.000	53.809
445.000	91.275	360.000	73.622	275.000	52.782
440.000	96.119	355.000	72.087	270.000	51.769
435.000	112.616	350.000	70.612	265.000	50.770
430.000	117.625	345.000	69.190	260.000	49.784
425.000	109.730	340.000	67.817	255.000	48.810
420.000	103.882	335.000	66.486	250.000	47.847
415.000	99.316	330.000	65.194	245.000	46.895
410.000	95.563	325.000	63.938	240.000	45.953
405.000	92.353	320.000	62.714	235.000	45.021

a relative maximum at $T = T^*$. Finally, note that $\bar{l}$ vs T curves for $0.99 < \gamma < 1$ are qualitatively similar to the $\gamma = 0.99$ curve and do not exhibit an infinite average lamellar thickness. The numerical integrations in the expressions for $\bar{l}^{(1)}(T)$ and $\bar{l}^{(3)}(T)$ could not be done for $\gamma \equiv 1$ as a result of the factor $(1 - \gamma)$ appearing in various denominators.

For comparison, we have reproduced part of Figure 3b of ref 1 as our Figure 3b, which shows the LH model $\bar{l}$ vs T curves with $\hat{\psi} = \psi$ for the selected values of $\psi = {}^1/_2, {}^3/_4$, 0.90, and 0.95. Some of the data which we calculated in order to construct these plots are given in Table VI. These LH model ψ curves exhibit the Δl catastrophe as Δf approaches $2\sigma/\psi a$, as do all LH curves for $0.95 < \psi \leq 1$. The curves for $0.95 < \psi \leq 1$ are similar to the $\psi = 0.95$ curve; since integrations can be done analytically in the

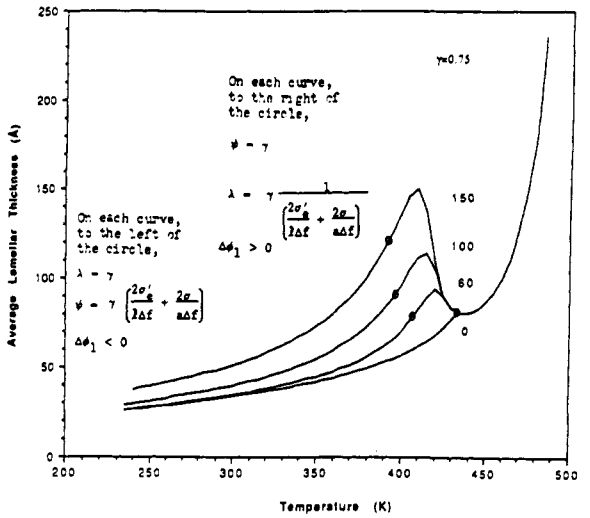

Figure 5. Plots of average lamellar thickness (Å) vs temperature (K) for $\sigma_e' = 0$, 60, 100, and 150 ergs/cm^2, each with $\theta = \gamma = {}^3/_4$. As in Figure 2, each open circle identifies the temperature T_0 at which $\Delta\phi_1(\bar{l},T) = 0$.

Table VI
Average Lamellar Thickness (Å) as a Function of Temperature (K) for $\psi = 0.90$ with $\hat{\psi} = \psi$, Reproduced from the Lauritzen–Hoffman (LH) Model[4,a]

temp (K)	LH $\phi = 0.90$	temp (K)	LH $\phi = 0.90$	temp (K)	LH $\phi = 0.90$
485.000	237.166	460.000	103.129	440.000	93.098
480.000	182.177	455.000	95.962	435.000	105.777
475.000	149.552	450.000	91.560	430.000	160.924
470.000	128.225	445.000	90.139	425.000	∞
465.000	113.507				

[a] Data are independent of σ_e'. See Figure 3b.

LH model when $\hat{\psi} = \psi$, $\bar{l}$ vs T for $\psi \equiv 1$ was able to be obtained.[1]

Thus, for high enough γ, our $\sigma_e' = 0$ model $\bar{l}$ vs T curves appear to have a break in slope at $T = T^*$. We suspect that there is indeed a break in slope at $T = T^*$ because the relation

$$\psi = \begin{cases} \gamma \dfrac{2\sigma}{a\Delta f} & \Delta f \geq 2\sigma/a \\ \gamma & \Delta f \leq 2\sigma/a \end{cases}$$

implies that $d\psi/dT$ is discontinuous at $\Delta f = 2\sigma/a$; however, we have not evaluated $d\bar{l}/dT$ at $\Delta f = 2\sigma/a$. The break in slope is apparently indiscernible up to γ values of about ${}^1/_2$, where the slope of $\bar{l}$ vs T has the same sign (positive) regardless of whether the point $\Delta f = 2\sigma/a$ is approached from values of Δf higher or lower than $2\sigma/a$. As γ increases, however, the break becomes pronounced with the concomitant appearance of a relative maximum in $\bar{l}$ at $T = T^*$ and a relative minimum in $\bar{l}$ at $T = T_*$; necessarily then, the slope of $\bar{l}$ vs T as Δf approaches $2\sigma/a$ from values less than $2\sigma/a$ becomes negative. We will refer to this undesirable behavior, manifest at high values of γ, as the $\bar{l}$ anomaly. Unlike the Δl catastrophe in the LH model, the relative maximum in $\bar{l}$ vs T, as noted above, always appears at $\Delta f = 2\sigma/a$ for all values of γ given that $\sigma_e' = 0$.

Next, we consider $\sigma_e' \neq 0$ for high values of γ. The $\bar{l}$ vs T curves for $\sigma_e' = 0$, 60, 100, and 150 ergs/cm^2—each with $\gamma = {}^3/_4$—are presented in Figure 5. The curves pass through a common relative minimum between $T = 440$ and $433^1/_3$ K (for which $\Delta f < 2\sigma/a$), and then each curve rises and passes through a relative maximum, that

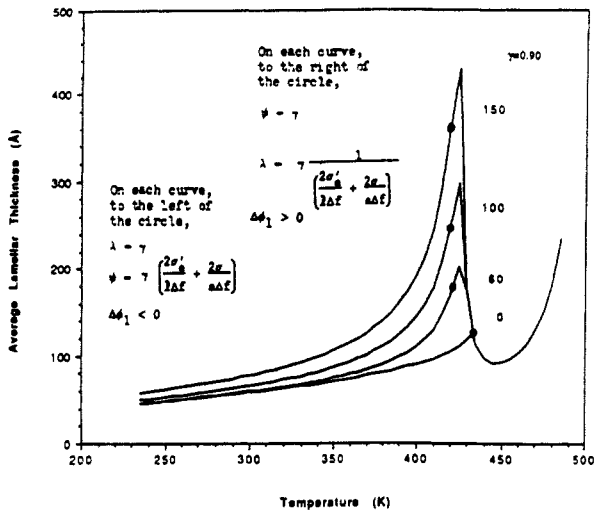

Figure 6. Plots of average lamellar thickness (Å) vs temperature (K) for $\sigma_e' = 0$, 60, 100, and 150 ergs/cm^2, each with $\theta = \gamma = 0.90$. As in Figure 2, each open circle identifies the temperature T_0 at which $\Delta\phi_1(\bar{l},T) = 0$.

maximum being relatively higher and occurring at higher Δf the larger the value of σ_e'. At each maximum, there would appear to be a break in the slope of $\bar{l}$ vs T. Having passed through its maximum, each curve decreases monotonically with decreasing T thereafter.

One should be careful to note that what appears to be a break in the slope of $\bar{l}$ vs T when $\sigma_e' \neq 0$ is probably not a break in slope; $d\bar{l}^{(2)}(T)/dT$ should be continuous for all relevant T. Whether a break in the slope of $\bar{l}$ vs T occurs at $\Delta f = 2\sigma/a$ when $\sigma_e' \neq 0$ as was presumed true for $\sigma_e' = 0$ cannot be determined conclusively from the appearance of the graphs, although the break appears to be absent.

Qualitatively similar $\bar{l}$ vs T curves are obtained for $\gamma = 0.9$ and $\sigma_e' = 0$, 60, 100, and 150 ergs/cm^2, as is shown in Figure 6. See also Table VII. The relative maxima are higher and "sharper" than the corresponding $\gamma = {}^3/_4$ curves, and they have moved to higher temperature. For $\gamma = 0.99$, the analogous curves, shown in Figure 7, exhibit $\bar{l}$ values which are unrealistically large as well as maxima which are extremely "sharp".

Thus, from the graphs, we see that the $\bar{l}$ anomaly becomes more pronounced but moves to higher temperature as γ increases for a fixed nonzero value of σ_e'. That is, although the relative maximum in $\bar{l}$ vs T can appear at some $\Delta f > 2\sigma/a$ when σ_e' is nonzero, the maximum becomes less pronounced as it moves to lower temperature upon a decrease in γ. Our model, then, does *not* fail at high supercooling but does exhibit anomalous behavior for temperatures corresponding to values of Δf "just" greater and "just" less than $2\sigma/a$. This undesirable behavior is pronounced for large values of γ and is more pronounced for larger values of σ_e' for a given γ.

We can easily rationalize mathematically how our calculated $\bar{l}$ vs T curves can rise with decreasing T for some $\Delta f > 2\sigma/a$ when σ_e' is nonzero. Recall that the expression for $\bar{l}^{(2)}(T)$, namely

$$\bar{l}^{(2)}(T) = \frac{\int_{l_1}^{l_0} lS_I(l,T)\,dl + \int_{l_0}^{\infty} lS_{II}(l,T)\,dl}{\int_{l_1}^{l_0} S_I(l,T)\,dl + \int_{l_0}^{\infty} S_{II}(l,T)\,dl}$$

contains two different integrands $S_I(l,T)$ and $S_{II}(l,T)$. Depending on σ_e', γ, and T, the contribution of the integrals involving $S_I(l,T)$ to $\bar{l}^{(2)}(T)$ may outweigh the contribution of the integrals involving $S_{II}(l,T)$, and, in some cases, our calculations show that to a very good approximation

$$\bar{l}^{(2)}(T) \approx \frac{\int_{l_1}^{l_0} lS_I(l,T)\,dl}{\int_{l_1}^{l_0} S_I(l,T)\,dl} \quad \text{with } l_0 \text{ approaching infinity}$$

But this is our expression for $\bar{l}^{(1)}(T)$ for the interval $\Delta f \leq 2\sigma/a$, and the results of our calculations using $\bar{l}^{(1)}(T)$ have been found to differ little from results using $\bar{l}^{(LH)}(T)$, i.e., the LH theory. Not unexpectedly then, $\bar{l}^{(2)}(T)$ can increase with decreasing T for some $\Delta f > 2\sigma/a$. We note that the numerator of $S_I(l,T)$, like the numerator of $S^{(LH)}(l,T)$, contains the factor $A_0 = e^{-\sigma'}e^{-bl(2\sigma-\gamma a\Delta f)/kT}$, the form of which has been associated with[10] increases in $\bar{l}$ with decreasing T.

Table VII
Average Lamellar Thickness (Å) as a Function of Temperature (K) for σ_e' = 60, 100, and 150 ergs/cm^2, Each with $\theta = \gamma = 0.90$ (See Figure 6)

temp (K)	$\sigma_e' = 60$	$\sigma_e' = 100$	$\sigma_e' = 150$
485.000	236.013	236.013	236.013
480.000	180.939	180.939	180.939
475.000	148.300	148.300	148.300
470.000	127.027	127.027	127.027
465.000	112.435	112.435	112.435
460.000	102.279	102.279	102.279
455.000	95.475	95.475	95.475
450.000	91.672	91.672	91.672
445.000	91.275	91.275	91.275
440.000	96.119	96.119	96.119
435.000	112.616	112.616	112.616
430.000	174.477	176.464	176.575
425.000	201.468	297.598	429.985
420.000	167.419	248.786	364.401
415.000	144.110	205.816	292.407
410.000	128.691	177.388	245.551
405.000	117.747	157.689	213.621
400.000	109.503	143.241	190.563
395.000	103.012	132.137	173.106
390.000	97.724	123.283	159.389
385.000	93.301	116.014	148.284
380.000	89.520	109.905	139.076
375.000	86.231	104.670	131.286
370.000	83.324	100.111	124.586
365.000	80.723	96.086	118.740
360.000	78.366	92.490	113.578
355.000	76.210	89.245	108.971
350.000	74.218	86.289	104.820
345.000	72.363	83.577	101.051
340.000	70.621	81.071	97.602
335.000	68.974	78.739	94.427
330.000	67.408	76.559	91.485
325.000	65.912	74.510	88.746
320.000	64.477	72.574	86.182
315.000	63.097	70.740	83.773
310.000	61.765	68.993	81.500
305.000	60.477	67.325	79.347
300.000	59.227	65.728	77.301
295.000	58.013	64.193	75.351
290.000	56.831	62.714	73.487
285.000	55.678	61.287	71.700
280.000	54.551	59.905	69.982
275.000	53.448	58.566	68.329
270.000	52.367	57.264	66.733
265.000	51.307	55.998	65.190
260.000	50.265	54.763	63.695
255.000	49.241	53.558	62.244
250.000	48.233	52.380	60.834
245.000	47.240	51.226	59.462
240.000	46.261	50.096	58.124
235.000	45.295	48.987	56.819

X. Conclusions

We have constructed a model of polymer crystallization which extends the LH theory by excluding negative free

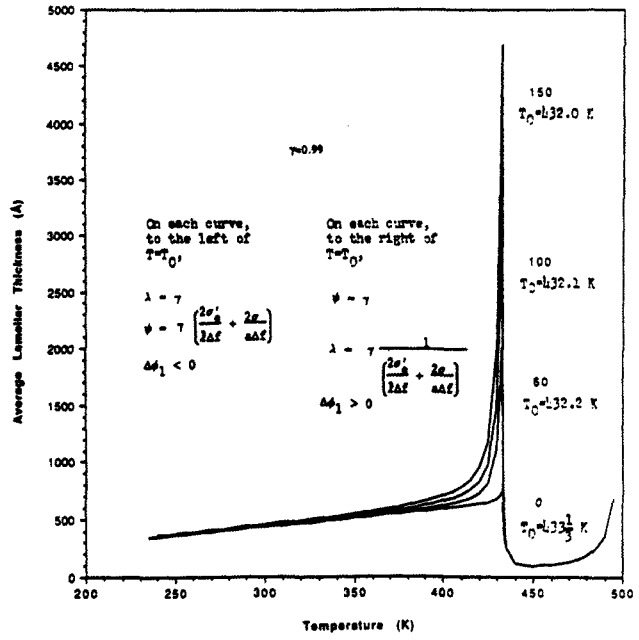

Figure 7. Plots of average lamellar thickness (Å) vs temperature (K) for $\sigma_e' = 0$, 60, 100, and 150 ergs/cm^2, each with $\theta = \gamma = 0.99$. For $\sigma_e' = 0$, 60, 100, and 150 ergs/cm^2, $T_0 = 433^1/_3$, 432.2, 432.1, and 432.0 K, respectively. As in Figure 2, T_0 is the temperature at which $\Delta\phi_1(\bar{l},T) = 0$.

energy barriers, and we have shown that the Δl catastrophe of the LH theory is related to the failure to exclude these negative barriers. Our results show that the new model is more consistent with experimental behavior at very high supercooling.

Our results with $\sigma_e' = 0$ clearly indicate that the $\bar{l}$ anomaly in our model—and in part the Δl catastrophe of the LH theory—are associated with the interval $\Delta f \leq 2\sigma/a$ and are thus connected to the expression $\Delta\phi_1 + E_1 = 2ab\sigma_e'$ $+ 2bl\sigma - \gamma abl\Delta f$. The $\bar{l}$ anomaly also appears to be connected to this expression even when $\sigma_e' \neq 0$, i.e., even when the maximum in $\bar{l}$ vs T occurs at a temperature for which Δf exceeds $2\sigma/a$. Although high values for γ and ψ are considered unrealistic as has been elucidated[6] recently, however, there is no guarantee that the LH theory as well as our extension of it has not failed to incorporate an as yet unknown constraint or feature which would improve the model results at high γ values. For example, high γ values may be unrealistic, but the $\bar{l}$ values for high γ from an improved model may simply be unrealistically large but nevertheless monotonically decreasing with decreasing T for all T.

In conclusion, we hope to extend our modification of the LH approach to polymer crystallization to treat the interesting systems which interact with an applied electric field.

References and Notes

(1) Scheinbeim, J. I.; Newman, B. A.; Sen, A. *Macromolecules* **1986**, *19*, 1454.
(2) Marand, H. L.; Stein, R. S.; Stack, G. M. *J. Polym. Sci., Polym. Phys. Ed.* **1988**, *26*, 1361.
(3) Marand, H. L.; Stein, R. S. *J. Polym. Sci., Polym. Phys. Ed.* **1989**, *27*, 1089.
(4) Lauritzen, J. I., Jr.; Hoffman, J. D. *J. Appl. Phys.* **1973**, *44*, 4340.
(5) Hoffman, J. D.; Davis, G. T.; Lauritzen, J. I., Jr. In *Treatise on Solid State Chemistry*; Hannay, N. B., Ed.; Plenum Press: New York, 1976; Vol. 3, Chapter 7, pp 497–614.
(6) Sanchez, I. C.; Di Marzio, E. A. *J. Chem. Phys.* **1971**, *55*, 893.
(7) Hoffman, J. D.; Miller, R. L. *Macromolecules* **1989**, *22*, 3038.
(8) Frank, F. C.; Tosi, M. *Proc. R. Soc. London* **1961**, *A263*, 323.
(9) Turnbull, D.; Fisher, J. C. *J. Chem. Phys.* **1949**, *17*, 71.
(10) *USER'S MANUAL-MATH/LIBRARY-FORTRAN Subroutines for Mathematical Applications*; IMSL, Inc.: Houston, TX, 1987; Chapter 4, pp 561–568.
(11) Hoffman, J. D.; Frolen, L. J.; Ross, G. S.; Lauritzen, J. I., Jr. *J. Res. Natl. Bur. Stand.* **1975**, *79A*, 671.
(12) Sanchez, I. C. *J. Macromol. Sci., Rev. Macromol. Chem.* **1974**, *C10*, 113–148.